AD-A037 674 YALE UNIV NEW HAVEN CONN DEPT OF ENGINEERING AND AP--ETC F/G 20/4
STRAIGHT DUCT SUPERSONIC DIFFUSER FLOW IN A LUDWIEG TUBE WITH U--ETC(U)
DEC 76 N ABUAF F44620-73-C-0032
UNCLASSIFIED SCIENTIFIC-6 AFOSR-TR-77-0201 NL

1 OF 1
ADA037674

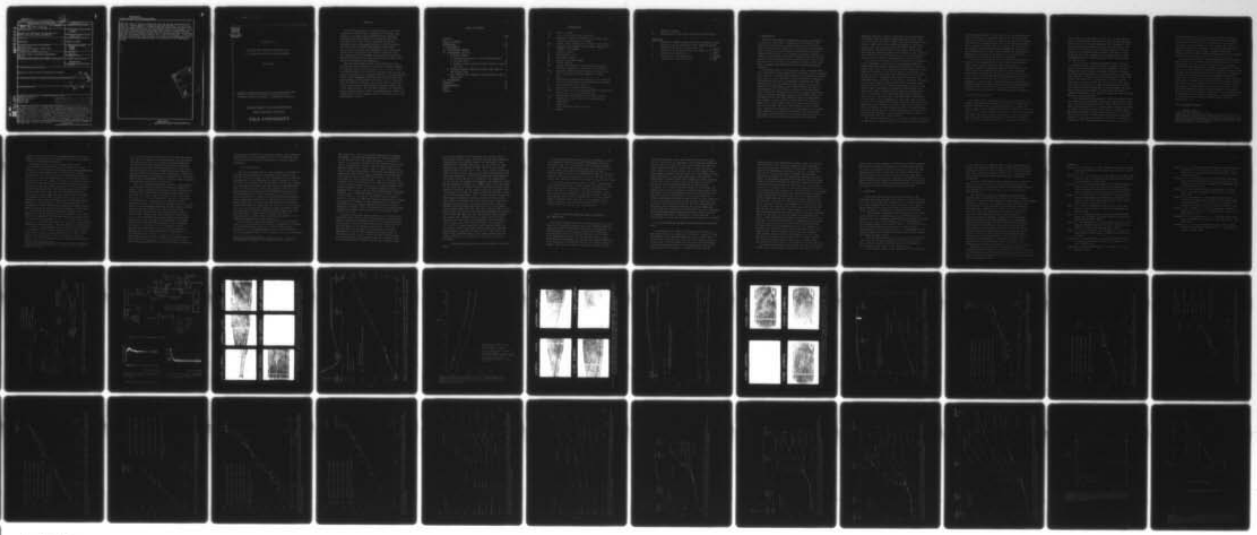

END

DATE
FILMED
4-77

UNCLASSIFIED

SECURITY CLASSIFICATION OF THIS PAGE (When Data Entered)

REPORT DOCUMENTATION PAGE

READ INSTRUCTIONS BEFORE COMPLETING FORM

1. REPORT NUMBER: AFOSR - TR - 77 - 0201	2. GOVT ACCESSION NO. / 3. RECIPIENT'S CATALOG NUMBER
4. TITLE (and Subtitle): STRAIGHT DUCT SUPERSONIC DIFFUSER FLOW IN A LUDWIEG TUBE WITH UPSTREAM DIAPHRAGM,	5. TYPE OF REPORT & PERIOD COVERED: INTERIM
	6. PERFORMING ORG. REPORT NUMBER: Report No 6
7. AUTHOR(s): NESIM ABUAF	8. CONTRACT OR GRANT NUMBER(s): F44620-73-C-0032
9. PERFORMING ORGANIZATION NAME AND ADDRESS: YALE UNIVERSITY, ENGINEERING AND APPLIED SCIENCE DEPT, NEW HAVEN, CT 06520	10. PROGRAM ELEMENT, PROJECT, TASK AREA & WORK UNIT NUMBERS: 2307/A3, 61102F
11. CONTROLLING OFFICE NAME AND ADDRESS: AIR FORCE OFFICE OF SCIENTIFIC RESEARCH/NA, BLDG 410, BOLLING AIR FORCE BASE, D C 20332	12. REPORT DATE: Dec 76
	13. NUMBER OF PAGES: 54
14. MONITORING AGENCY NAME & ADDRESS (if different from Controlling Office): Scientific - 6	15. SECURITY CLASS. (of this report): UNCLASSIFIED
	15a. DECLASSIFICATION DOWNGRADING SCHEDULE

16. DISTRIBUTION STATEMENT (of this Report)

Approved for public release; distribution unlimited.

17. DISTRIBUTION STATEMENT (of the abstract entered in Block 20, if different from Report)

18. SUPPLEMENTARY NOTES

19. KEY WORDS (Continue on reverse side if necessary and identify by block number)

DIFFUSERS, SUPERSONIC
PRESSURE RECOVERY
WIND TUNNELS
LUDWIEG TUBE

20. ABSTRACT (Continue on reverse side if necessary and identify by block number)

The starting process of supersonic flow in a nozzle followed by constant area, straight duct diffusers was studied in a Ludwieg tube equipped with an upstream diaphragm. The time required to establish steady flow from rest at the exit of the supersonic nozzle was determined from shadowgraph pictures of the flow field, and from static pressure measurements. The initial pressure ratios across the diaphragm to start the supersonic flow at the nozzle exit are also reported. They are compared with the minimum pressure ratio required to sustain the flow at the nozzle exit during the first flow cycle of the Ludwieg tube operation. The

DD FORM 1 JAN 73 1473 EDITION OF 1 NOV 65 IS OBSOLETE

UNCLASSIFIED

SECURITY CLASSIFICATION OF THIS PAGE (When Data Entered)

flow Mach number is M=2.8 and nozzle exit area and diffuser cross section are (1x2) in^2. Various lengths of diffusers were used with L/D=0, 1.5, 3, 4.5, 6. Within the range ($2.8x10^5$ to $1.7x10^6$) of Reynolds numbers, Re_D, as based on the nozzle exit hydraulic diameter, the experimental results were unchanged. Starting times at the nozzle exit with boundary layer suction to remove 2% of the total mass flow rate applied through a slit at the nozzle exit were 16-33% lower than the ones obtained without suction, for a 3 inch long diffuser. For the same diffuser, the limiting initial pressure ratio across the diaphragm that allows the smooth start of the supersonic flow at the nozzle exit, was unchanged by section.

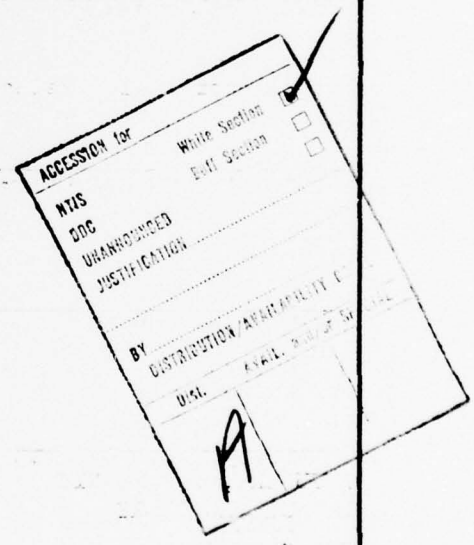

December 1976

STRAIGHT DUCT SUPERSONIC DIFFUSER FLOW IN A LUDWIEG TUBE WITH UPSTREAM DIAPHRAGM

Nesim Abuaf

Scientific Report #6 prepared for AFOSR Research Grant F44620-73-C-0032 "Supersonic Diffuser Research".

DEPARTMENT OF ENGINEERING
AND APPLIED SCIENCE

YALE UNIVERSITY

ABSTRACT

The starting process of supersonic flow in a nozzle followed by constant area, straight duct diffusers was studied in a Ludwieg tube equipped with an upstream diaphragm. The time required to establish steady flow from rest at the exit of the supersonic nozzle was determined from shadowgraph pictures of the flow field, and from static pressure measurements. The initial pressure ratios across the diaphragm to start the supersonic flow at the nozzle exit are also reported. They are compared with the minimum pressure ratio required to sustain the flow at the nozzle exit during the first flow cycle of the Ludwieg tube operation.

The flow Mach number is M=2.8 and nozzle exit area and diffuser cross section are (2x2) in^2. Various lengths of diffusers were used with L/D=0, 1.5, 3, 4.5, 6. Within the range (2.8×10^5 to 1.7×10^6) of Reynolds numbers, Re_D, as based on the nozzle exit hydraulic diameter, the experimental results were unchanged. Starting times at the nozzle exit with boundary layer suction to remove 2% of the total mass flow rate applied through a slit at the nozzle exit were 16-33% lower than the ones obtained without suction, for a 3 inch long diffuser. For the same diffuser, the limiting initial pressure ratio across the diaphragm that allows the smooth start of the supersonic flow at the nozzle exit, was unchanged by suction.

TABLE OF CONTENTS

NOMENCLATURE

a	speed of sound
A	area, nozzle exit area $=(2x2)$ in^2
D	hydraulic diameter at nozzle exit (4 times area divided by perimeter), =2 inches
h^*	height of the nozzle at the throat, =0.472 inches
ℓ	characteristic length of the nozzle, defined as $\sqrt{R^*h^*}$ = 1.89 inches
L	diffuser length
M	Mach number, = v/a
M_s	shock Mach number
$\bar{M}_s$	average shock Mach number
p	static pressure
R^*	radius of curvature of the diverging section of the nozzle contour at the throat, =7.64 inches
Re_D	Reynolds number based on hydraulic diameter and test section free stream parameters, $=v\rho D/\mu$
t	time
t_c	time interval between the arrival of the shock at the nozzle throat and the occurrence of the spark
t_s	total starting time, $=t_{s1}+t_{s2}$
$\bar{t}_s$	dimensionless starting time, $=t_s/\tau_f$
t_{s1}	time elapsed from the diaphragm rupture until shock wave arrives at a specific location
t_{s2}	time between the arrival of the shock and the attainment of the steady free stream pressure
T	temperature
v	flow speed
x	axial distance, nozzle exit x=0
ρ	density

μ	dynamic viscosity
τ_f	characteristic flow time, defined by $\ell/a^*=0.153$ ms

Subscripts

1	downstream initial conditions before diaphragm rupture	
4	upstream initial conditions before diaphragm rupture	
3	conditions upstream of nozzle after the expansion fan has passed into the supply tube	during first cycle of the Ludwieg tube flow
o	nozzle supply conditions	
n	conditions at the nozzle end	
d	conditions at the diffuser end	

I. INTRODUCTION

With the development of gasdynamic lasers, new interest has arisen in the study of supersonic flow diffusers. The steady state performance characteristics such as pressure recovery and diffuser length for optimum recovery of straight duct, constant area and variable area diffusers, were most recently investigated at our laboratory by Merkli (1975a, b, 1976) in a continuous wind tunnel. Starting times and initial pressure ratios needed to start supersonic flow at the nozzle exit have also been reported by Merkli and Abuaf (1976) who used a Ludwieg tube with upstream and downstream diaphragm locations.

The Ludwieg tube, or the tube wind tunnel (Ludwieg 1955), is an intermittent wind tunnel where the supply tank is replaced by a long tube. A converging-diverging nozzle generating supersonic flow in a test section is located between the upstream and downstream sections. A diaphragm, separating the high pressure side (p_4, T_4) from the low pressure one (p_1, T_1), before flow is initiated, can be placed either upstream or downstream of the test section. Ludwieg used a downstream valve and Hottner (1965) was the first to conduct experiments with an upstream diaphragm location. Falk (1963), Falk and Hertzberg (1967), and Falk (1968) presented an approximate wave diagram for the starting process where the nozzle was replaced by a zero length section, followed by a constant area test section. Davis and Gwin (1967) and Davis (1968) gave a similar wave diagram for the flow process in a Ludwieg tube. Moreover they reported experiments with an upstream diaphragm location resulting in starting times that were 55 per cent shorter than those obtained with a downstream

diaphragm location. Figure 1 represents the wave diagram of the Ludwieg tube flow after diaphragm rupture after Davis and Gwin (1967) and Miller (1968). The general nature of the flow as indicated in this simplified diagram is basically correct, but the wave process in the throat region is in reality more complicated due to reflections of the shock wave from the converging walls of the nozzle. A more detailed wave analysis of the starting process is in fact needed to predict a more realistic wave diagram of the flow field.

The flow in the Ludwieg tube is initiated by the rupture of the diaphragm. In the case of an upstream diaphragm a backward-facing centered expansion fan propagates into the supply tube. This fan is reflected off the closed end of this tube and it returns to the nozzle throat. This process is called the first flow cycle. The expansion wave sets the gas in motion and it slightly lowers the local pressure and temperature (p_3, T_3) ahead of the nozzle. Since the flow speed in the nozzle supply after passage of the expansion fan is low, $p_3 = p_o$ and $T_3 = T_o$, where the subscript o refers to the nozzle supply conditions in analogy to conventional supersonic wind tunnels. Expressions relating all properties of the gas during the first flow cycle have been derived by Cable and Cox (1963) and Davis and Gwin (1967). Subsequent to the rupture of the diaphragm, a shock wave and a contact surface proceed downstream through the nozzle and test section. Additional waves follow the contact surface that separates the gas initially in the supply tube and the downstream tube, to adjust the nozzle test section pressure to the freestream pressure corresponding to the design Mach number expected at the nozzle exit for a given nozzle.

The total starting time, t_s, at a fixed location is defined as the time that elapses between the rupture of the diaphragm

and the establishment of steady flow, i.e. constant pressure at that location. The starting time is the sum of two time intervals as noted in Figure 1. For one t_{s1} gives the elapsed time from the diaphragm rupture until the shock wave arrives at the specific location, and t_{s2}, denotes the time between the arrival of the shock and the attainment of the steady free stream pressure. This total starting time definition is dependent on location. At each point of the flow field a different total starting time will be recorded.

In the present report we have investigated the starting process of the supersonic flow at the nozzle and diffuser exits respectively by means of spark shadowgraph pictures in which the different phases of the flow can be seen. The results compare well with the static pressure measurements performed at the same locations. The results of the flow starting times and corresponding initial pressure ratios needed to start the flow at the nozzle exit, are extended to a wider range of initial upstream pressures and Reynolds numbers than the results previously reported (Merkli and Abuaf 1976). Moreover the effects of boundary layer suction at the nozzle exit on starting time was determined.

II. EXPERIMENTAL METHODS

The experimental investigation was conducted in the Yale Ludwieg tube which was described in detail in our last report (Merkli and Abuaf 1976). The upstream tube (5.3 inches ID, 22 feet long) and the downstream tube (3.76 inches ID, 25 feet long, ~ 2 ft^3) sections respectively have 90° bends to accommodate the total tube length within the confines of the laboratory (Fig. 2a). The downstream section was connected to a dump tank (17 ft^3) to reduce the effect of shock wave reflections.

The 24 inch long test section, (2x5) in^2, is connected to both the upstream and downstream sections by two transition pieces. For the reported experiments the diaphragm (3 mil Mylar sheets) was located at the upstream end of the test section (1.81 inches from the nozzle entrance). The diaphragms were scratched along diagonal lines with a razor blade and they were ruptured by an X-shaped cutter. This preparation prevents diaphragm pieces from flying through the test section.

A 12 inch long converging-diverging nozzle is placed in the test section, leaving another 12 inches of test section for the installation of various diffusers. The two-dimensional nozzle contour was based on method of characteristics calculations for a uniform M=3 flow at the nozzle exit without a boundary layer correction (Merkli 1976). The throat, (0.472x2) in^2, is located at 4 inches from the nozzle inlet and the nozzle exit area is (2x2) in^2. Metal side walls with holes at 1 inch intervals along the flow axis allow pressure measurements to be performed. For these static pressure measurements Kistler Model 606L quartz pressure transducers (rise time 3 μs) are used with a Kistler Model 504 charge amplifier.

After placing the diaphragm, in a typical experiment both the upstream and downstream sections are pumped down to a few torr. The upstream section is next filled with dry air (dew point better than 213 K) to a given initial upstream pressure, p_4, which is measured either by a Wallace & Tiernan Model FA145 pressure gauge (0-120 inches of mercury, ± 0.2 inches Hg) or by a Wallace & Tiernan Type FA187 mercury manometer, capable of measuring an accuracy of 0.1 torr in a range of 0-800 torr. The initial downstream pressure, p_1, is next set

to the required value by bleeding air from the atmosphere and it is measured by Wallace & Tiernan Model FA160 gauges (0-100 torr or 0-400 torr). The breaking of the diaphragm initiates the flow through the test section. The output of a pressure transducer located at the nozzle entrance (x=-11 inches) triggers a four channel storage oscilloscope (Tektronix Model 5103N). Typical oscillograms of the pressure variation as a function of time are given in Fig. 2b.

Two plexiglass windows allowed shadowgraph and schlieren observations of the entire nozzle-diffuser flow area. For the shadowgraph pictures of the flow field a spark source was used with a collimating lens (4 inches in diameter) as noted in Fig. 2a. The output of a pressure transducer located at the throat* and sensing the arrival of the shock wave, triggered a Hewlett Packard 5233L electronic counter and a General Radio Corp. Type 1392-A time delay generator. After a preset time delay, an output from the time delay generator triggered the short duration high voltage (1 μs, 7500 v) spark source. The output of a light sensitive phototransistor was used to stop the electronic counter at the occurrence of the spark. Thus the time period between the arrival of the starting shock at the nozzle throat and the recording of the photograph can be directly read from the electronic counter within an accuracy of 1 μs.

III. EXPERIMENTAL RESULTS

1. STARTING PROCESS

* The pressure transducer to trigger the counter and the time delay generator was located at the throat because at that location a well defined shock wave and pressure pulse appear. This scheme eliminates the uncertainties involved in the non-reproducible breaking of the diaphragm.

When the upstream diaphragm of a Ludwieg tube is ruptured a wave pattern as presented in Figure 1 develops in the nozzle followed by the straight duct diffuser. The present experimental results generally agree with this picture.

A. Shadowgraph pictures of the starting process

Subsequent to the rupture of the diaphragm a shock wave travels along the nozzle-diffuser duct (Fig. 1). This fact is observed in the typical shadowgraphs presented in Fig. 3 taken at different locations and times. An upstream supply pressure, p_o=966 torr, an initial downstream pressure, p_1=150 torr, were used with the nozzle followed by a 6 inches long diffuser of constant cross section. The photographs are given at full scale. The vertical solid black lines* are strings attached at reference points along the test section in order to determine the location of the shock wave. The first picture shows the pressure transducer located at the throat and the last picture in the sequence depicts the shock leaving the end of the diffuser. The boundary layer estimated to be less than 0.09 inches at the nozzle exit for the present experimental conditions is not visible in the pictures. The x-t diagram for the shock wave, for the initial pressure ratio, p_4/p_1=6.67 is presented in Fig. 4 as obtained from similar shadowgraph pictures. In the same figure, a theoretical curve is plotted for comparison. First an initial shock Mach number was calculated for the given pressure ratio, p_4/p_1=6.67, by using the following relationship (Glass and Hall 1959)

$$p_4/p_1 = 1/6\ [7M_s^2-1].[1-1/6(M_s-1/M_s)]^{-7} \ ,$$

---

* All the extra lines present in the picture are caused by scratches on the plexiglass windows.

valid for the case of air/air and a constant area shock tube. The variation of the shock Mach number with the cross sectional area as it travels through the converging-diverging nozzle was taken into account by the following expression (Chisnell 1957, Whitham 1958)

$$\frac{dA}{A} = - \frac{2\ M_s}{(M_s^2-1)} \cdot \frac{dM_s}{K(M_s)}$$

An expression for the function $K(M_s)$ is given in the above references. The x-t diagram for the shock wave is drawn knowing the speed of sound for T_1=296 K and the variation of the shock Mach number, M_s, along the nozzle. The experimental results recorded downstream of the throat agree well with the theoretical predictions with a maximum deviation of 12 %.

Shadowgraph pictures were also taken in the vicinity of the 6 inch diffuser exit for various initial pressure ratios, p_4/p_1, recording the location of the shock wave and the time it took for the shock wave to travel from the nozzle throat to the specific location. This provided an average experimental shock wave Mach number, $\bar{M}_s$. The results are depicted in Fig. 5 where a solid line gives the shock Mach number as predicted by the constant area shock tube theory (Glass and Hall 1959). Moreover a dashed line gives an average shock Mach number calculated by taking into account the area change along the nozzle (Whitham 1958). As observed in Fig. 6, the experimental results show scatter, however they are still within ± 10 % of the latter predictions. The experimental average shock Mach numbers are lower than the predicted ones for the low pressure ratios. Conversely they are higher for the higher ones. The speed of the diaphragm rupture depends strongly on the initial pressure ratio. Since the nozzle

entrance is very close to the diaphragm location (at 1.81 inches), the effect of the diaphragm rupture will therefore affect the experimental results.

According to Fig. 1, the upstream facing wave* the interface will adjust the pressure level at a given location to the steady free stream pressure which corresponds to the local Mach number. Fig. 6 presents four typical shadowgraphs taken with $p_4/p_1=6.67$ at different times for the same test section configuration. The pictures show the upstream facing wave which is formed by the effects on the flow by the interaction of the initial pressure ratio and the local steady free stream pressure. The wave as expected becomes stronger and thus more visible downstream of the nozzle throat. This wave moves then downstream and stops at a given location along the test section which is mainly determined by the initial pressure ratio, p_4/p_1. The x-t diagram for this wave as obtained from similar shadowgraph pictures is shown in Fig. 7. The time measured here, t_c, corresponds to the time interval between the arrival of the shock at the nozzle throat and the occurrence of the spark, i.e. the instant at which the picture is taken. The x-t diagram for the starting shock is also plotted on the same figure for comparison. The results agree qualitatively with the wave pattern presented in Fig. 1. At this stage, these results for the upstream facing wave can not be compared with a theoretical curve, since no such calculations are available.

A series of shadowgraphs taken at the exit of the nozzle as a function of time are presented in Fig. 8. The vertical black line is again a string attached at 0.2 inches downstream of the nozzle exit. First the shock is observed, then at 3 ms some disturbances pass through, and finally at

---

* By an upstream facing wave, we mean a Q shock moving downstream and being accompanied by a local pressure decrease after its passage.

4 to 7 ms the upstream facing wave has reached the nozzle exit and it is observed to oscillate back and forth about the flow direction at that location. Steady supersonic flow with free stream conditions follows this upstream facing wave. The wave system, following the initial shock wave and ending with the upstream facing wave, appears as oblique shocks at the nozzle exit, followed by a series of shock waves within the diffuser. Deceleration of the flow, adverse pressure gradient effects, boundary layer separation and turbulent mixing are also observed.

When the upstream facing wave reaches a given location in the nozzle-diffuser assembly oscillating around that point, steady supersonic flow ceases at that location and the flow breaks down (Merkli and Abuaf 1976). When the upstream facing wave stays downstream of the nozzle exit for $p_4/p_1 > 6.67$ steady supersonic flow exists throughout the nozzle and it is followed by a slowing down and pressure increase in the diffuser through a series of shock waves. The corresponding pressure rise yields the pressure recovery and the length of the shock system in the diffuser is called the pressure recovery zone (Merkli 1975a, 1976). Varying the initial pressure ratio, p_4/p_1, for a 6 inch diffuser, the location where the upstream facing wave stops, and where the supersonic flow breaks down in the nozzle-diffuser assembly can be determined (see Fig. 9). For $p_4/p_1 > 10.1$, supersonic flow is observed throughout the entire test section with the familiar over- and under-expanded jet configurations at the diffuser exit. For $10.1 > p_4/p_1 > 6.67$, the disturbance moves from the diffuser end upstream towards the nozzle end. For $p_4/p_1 < 6.67$ the shock wave system moves further upstream into the nozzle. Since the upstream

facing wave is observed to oscillate around a given location, the limiting line as presented in Fig. 9 for the break down of the flow will in reality be given by a broader range of conditions.

B. Starting times

The total starting time at a given location is defined as the time period required to establish steady flow at that location after the rupture of the diaphragm. As discussed, the breaking time of the diaphragm is erratic and thus a source of error. To eliminate this uncertainty in shock tube research, it is customary to assume that this time is negligibly small (Fig. 1). The previous section was concerned with the time period between the rupture of the diaphragm and the arrival of the shock wave at a given location, t_{s1}. Its variation was investigated as a function of the experimental parameters and an approximate method for its prediction was presented. This section will deal with the time required to establish steady flow after the shock wave has arrived at that location, i.e. t_{s2}. The results are similar to those presented in the previous report by Merkli and Abuaf (1976) except that they are extended to a wider range of supply pressures or Reynolds numbers based on the properties calculated for the free stream conditions at the nozzle exit.

Fig. 10 depicts the second period of the flow starting time, t_{s2}, at the nozzle exit without a diffuser as a function of the pressure ratio, p_1/p_o for various nozzle supply pressures, p_o or Reynolds numbers, Re_D *. The wide scatter of the experimental data is not caused by errors in measurement

---

*Here the length entering the Reynolds number is defined as the hydraulic diameter of the nozzle exit, D=2 inches.

but rather it is due to the erratic breaking of the Mylar diaphragms. This scatter diminishes for the data recorded at the diffuser exit for longer diffusers. The starting times, t_{s2}, increase linearly with the pressure ratio, p_1/p_o, and it is independent of the upstream supply pressure or Reynolds number for $2.8 \times 10^5 < Re_D < 7.2 \times 10^5$. The vertical line at the right hand side of the figure corresponds to the limiting pressure ratio, p_1/p_o, for which the steady supersonic flow at the nozzle exit was disturbed. Figs. 11 and 12 present the flow starting times, t_{s2}, at the nozzle and diffuser exits respectively for a 3 inch long diffuser. Figs. 13 and 14 depict similar results for a 6 inch diffuser. Here too the starting times, t_{s2}, increase linearly with the pressure ratio, p_1/p_o, and they are independent of the supply pressure, p_o, or Reynolds number, Re_D, for $3.8 \times 10^5 < Re_D < 1.7 \times 10^6$. Figs. 15, 16 and 17, 18 finally present similar data for a 9 and a 12 inch long diffuser respectively. Fitting a straight line through the experimental data of each case by means of a least square analysis provides the results tabulated in Tables I and II respectively. The straight lines obtained from these expressions are the solid lines shown in Figs. 10 to 18.

A cross plot of the starting times, t_{s2}, for the flow at the nozzle and diffuser exits respectively as a function of diffuser length for a constant value of the initial pressure ratio, p_1/p_o, gives the curves presented in Figs. 19 and 20. For low values of the pressure ratio, $p_1/p_o < 0.05$ the starting time for the flow at the nozzle exit is nearly independent of the diffuser length. For higher values of the pressure ratio, $p_1/p_o > 0.075$, the flow starting times at the nozzle exit, t_{s2}, increase with the diffuser length. Fig. 20 depicting the variation of the flow starting times,

t_{s2}, at the diffuser exit shows that for a given value of the pressure ratio, p_1/p_o, the flow starting times increase linearly with the diffuser length. The variation of the dimensionless starting times, $\bar{t}_{s2} = t_{s2}/\tau_f$, with the axial distance, x/D, are plotted in Figs. 21 to 24 for various length diffusers, L/D= 1.5, 3, 4.5, and 6, and for different values of the pressure ratio, p_1/p_o. The characteristic flow time here defined by $\tau_f=\ell/a^*$, is related to the geometry of the nozzle throat and it is a measure of the acceleration of the flow or its cooling rate (Wegener and Cagliostro 1972). The characteristic length, ℓ, $=\sqrt{R^*h^*}$, where h* is the height of the nozzle at the throat (h*=0.472 inches), and R* is the radius of curvature of the nozzle profile at the throat (R*= 7.64 inches). The speed of sound at the sonic throat is given by a*. At locations where $x/D < -3$ the pressures recorded by the pressure transducers show an increase in the pressure level above the initial value with the arrival of the shock. The pressure overshoots its steady state level, reaches a maximum, and then drops down and levels off at its steady state running value (see Fig. 2b). The starting time, t_{s2}, at those points was taken as the time period between the arrival of the shock and the first time the pressure level reached the steady state running value. In this region the flow starting times are seen to be independent of the pressure ratio, p_1/p_o, and of the diffuser length. In the region $-3 < x/D < -2$ a sharp increase in the starting times, t_{s2}, is observed. This is the same location where the upstream facing wave was observed in Figs. 6 and 7. This region is seen to move upstream closer to the nozzle throat for the longer diffusers, i.e. from x/D=-2 for L/D=1.5 to x/D=-3 for L/D=6.

C. Minimum initial pressure ratios needed to start the flow.

The initial pressure ratios, p_o/p_1, sufficient to start the supersonic flow at the nozzle and diffuser exits are plotted in Fig. 25 as a function of the diffuser length, $0 < L/D < 6$. The pressure ratios, p_o/p_1, that start the flow at the nozzle exit, show a minimum ($p_o/p_1=5.2$) once a diffuser length of $L/D=4.5$ is attained. In turn the optimum pressure ratio, p_o/p_1, sufficient to start the flow at the nozzle exit without a diffuser is equal to $p_o/p_1=10.3$ (± 10%).

It is interesting to note that no change of the needed starting pressure ratio for the nozzle exit without a diffuser occurs when diffusers of varying length are added whose exit flow is supersonic. In fact the diffuser acts here like an extended parallel wall test section. The present results agree with the conclusions of our last report (Merkli and Abuaf 1976) and they are independent of the Reynolds number in the restricted range $2.8\times10^5 < Re_D < 1.7\times10^6$ which was used in this investigation.

2. PRESSURE RECOVERY DURING THE FIRST FLOW CYCLE OF THE LUDWIEG TUBE

The static pressure levels at the diffuser exit, p_d, for diffusers of different lengths were also recorded during the first flow cycle of the Ludwieg tube while operating at the limiting pressure ratios, p_o/p_1. Under these conditions the supersonic flow at the nozzle exit was just starting to be disturbed (see Fig. 25). The pressure ratio, p_o/p_d, which should correspond to the steady state pressure recovery of the diffuser, is plotted in Fig. 26 for various diffuser lengths. The pressure levels at the diffuser exits showed

violent fluctuations with time during the first flow cycle (up to ± 20-30 % of p_d) leading to the uncertainty indicated by the error bars (Fig. 26). The square symbol presents the point obtained by Merkli (1976) with a steady continuous wind tunnel for a similar nozzle and for the boundary layer displacement parameter δ^*/D of about 0.04. The current results agree with those of the continuous tunnel. The pressure fluctuations at the diffuser exit during the steady operation in the first cycle at the pressure ratio when the flow at the nozzle exit is breaking down may be caused by the following. For one,the operation period of the Ludwieg tube (first cycle) is not as steady as predicted from theory since variations of the downstream pressure by reflection of waves may cause pressure fluctuations. It is well known that close to optimum performance diffuser flows are very sensitive to small disturbances. Secondly the pressure variations may be due to adverse pressure gradient effects. Boundary layer separation and turbulent mixing may be carried downstream to the transducer location at the diffuser exit. The continuous wind tunnel experiments (Merkli 1976) were carried out with a Statham gauge which is insensitive to fast pressure fluctuations and thus the fluctuations may have been overlooked.

3. FLOW STARTING WITH BOUNDARY LAYER SUCTION AT THE NOZZLE EXIT.

To investigate the effect of boundary layer suction at the nozzle exit on the starting of the flow, a special 3 inch long diffuser block was designed (see Fig. 2a lower left). A suction slit consisting of a (3/16x1.5) in^2 opening located at the nozzle exit was added. The dump tank was disconnected from the downstream section of the Ludwieg tube and the 90^o bend-T piece was replaced by a simple 90^o bend. The new

diffuser blocks were connected by copper tubing (1 inch ID, 7 feet long) to the dump tank through a second diaphragm and a pin mechanism. To conduct an experiment, the initial upstream and downstream pressures, p_4 and p_1, respectively were set to the required value following the procedure described in Chapter II. The large dump tank was evacuated. First, the diaphragm separating the dump tank from the copper tubing leading to the diffuser block was ruptured in order to intiate suction through the slit. Next the upstream diaphragm of the Ludwieg tube was ruptured manually starting the flow through the test section. The flow was assumed to be choked at the diffuser suction slit. For a given gas and a constant supply temperature, the mass flow rate, $\dot{m}$, is proportional to the throat area and the supply pressure for choked flow. The pressure at the exit of the nozzle during the first flow cycle is about 35 torr, (corresponding to a supply pressure, p_o, of 966 torr), and the area of the two slits is 0.56 in^2. The suction mass flow rate is thus around 2 % of the total mass flow rate through the nozzle in the first cycle. Starting times for the flow, t_{s2}, at the nozzle and diffuser exits with a 3 inch diffuser and suction are presented in the last two Figs. 27 and 28 respectively as a function of the initial pressure ratio, p_1/p_o. It is clear that the starting times at both locations are reduced by 16 to 33 % by suction for the high and low values of the initial pressure ratio, p_1/p_o, respectively, when we compare them to the flow starting times without suction at the same location. For the 3 inch diffuser the boundary layer suction did not seem to affect the limiting initial pressure ratio, p_1/p_o, which caused the steady supersonic flow at the nozzle exit to be disturbed.

One problem encountered during these runs was the sequence of the timing between the initiation of the suction at the

nozzle exit and the starting of the flow in the test section. Two diaphragm breaking mechanisms were needed whose opening periods are reproducible with an accuracy of 1 ms. Thus the expansion fan of the suction and the initial shock wave of the main flow arrive at the nozzle exit at the same time. The repeatability could not be improved to better than 10 ms unless a new design would have been introduced. Thus in some experiments the set initial downstream pressure was observed to change even before the Ludwieg tube flow started.

IV. CONCLUSIONS

1. The starting time period from the rupture of the diaphragm until the arrival of the shock at a given location, t_{s1}, can be predicted with an accuracy of ± 10% by predicting the shock strength from the initial pressure ratio, p_4/p_1, and by taking into account the effect of area change on the shock strength as it propagates through the test section.

2. The starting time period from the arrival of the shock until steady flow is established, t_{s2}, at the nozzle and diffuser exits; i) increases linearly with the initial pressure ratio, p_1/p_o, for a given diffuser, ii) is independent of the Reynolds number in the range 2.8×10^5 to 1.7×10^6, and iii) for the initial pressure ratio $p_1/p_o < 0.05$, the flow starting time at the nozzle exit, t_{s2}, is independent of the diffuser length, but increases linearly with diffuser length for higher pressure ratios.

3. The initial pressure ratio, p_o/p_1, to start the supersonic flow at the nozzle exit shows a minimum ($p_o/p_1 = 5.2$) for a diffuser length of L/D=4.5, and it is independent of the Reynolds number, Re_D, in the range quoted.

4. The pressure ratio, p_o/p_d, during the first flow cycle

of the Ludwieg tube, corresponding to the pressure recovery through the diffuser, shows a minimum value (p_o/p_d=4.45) for a diffuser length of L/D=4.5. These results are in agreement with those obtained by Merkli (1976), L/D ~ 6 and p_o/p_d=4.2, in a continuous wind tunnel under similar experimental conditions.

5. For a 3 inch diffuser with boundary layer suction to remove 2% of the total mass flow rate through the nozzle applied through a slit at the nozzle exit appreciably reduced the starting times for the flow, t_{s2}, at the nozzle and diffuser exits.

The supersonic diffuser performance characteristics observed can be summarized as follows. First the simplest geometry of constant area emerged as quite attractive, efficient, and easy to construct. The supersonic flow starting times at the nozzle exit are shorter for an upstream diaphragm location than a downstream one. These starting times can still be reduced by boundary layer suction at the nozzle exit. The flow starting process can in principle be predicted from wave diagrams existing in the literature. One disadvantage of this configuration is the diaphragm material flying through the test section which can disturb the starting flow field, but this can be eliminated by proper design considerations. The initial pressure ratios needed to start the supersonic flow throughout the nozzle are not affected by the location of the diaphragm. The optimum pressure recovery during steady operation and the diffuser length required to obtain this recovery can be predicted once the Mach number and the boundary layer displacement parameter are known at the exit of the nozzle.

Although we are far from a complete understanding of supersonic diffuser flows, the experimental findings reported are providing some basic points to consider in the choice and design of supersonic diffusers, for some specific applications such as gasdynamic lasers.

REFERENCES

Cable, A. J. and Cox, R. M., "The Ludwieg Pressure-tube Supersonic Wind Tunnel", Aeron. Quart., vol. XIV, 2, pp.143-157, 1963.

Chisnell, R. F., "The Motion of a Shock Wave in a Channel,with Applications to Cylindrical and Spherical Shock Waves", J. Fluid Mech., 2, 286, 1957.

Davis, J. W., "A Shock Tube Technique for Producing Subsonic, Transonic and Supersonic Flows with Extremely High Reynolds Numbers", AIAA Paper No. 68-18, presented at AIAA 6th Aerospace Sciences Meeting, New York, 1968.

Davis, J. W. and Gwin, H. S., "Studies of a Short Duration High Reynolds Number Tube Wind Tunnel Concept", presented at the 27th semi-annual meeting of the Supersonic Tunnel Association, 1967.

Falk, T.J., "An SST Aerodynamic Test Facility Using Short Duration Flow Techiques", Cornell Aeronautical Lab. Report, 1963.

Falk, T. J., "A Tube Wind Tunnel for High Reynolds Number Supersonic Testing", Aerospace Research Laboratories, Report ARL-68-0031, 1968.

Falk, T. J. and Hertzberg, A., "A Tube Wind Tunnel for High Reynolds Number Supersonic Testing", Report No. AD-2297-A-1, Cornell Aeronautical Lab., 1967.

Glass, I. I. and Gordon Hall, J., "Handbook of Supersonic Aerodynamics. Shock Tubes", NAVORD Report 1488, vol. 6, 1959.

Hottner, Th., "Untersuchungen an einem Modell-Rohrwindkanal bei Machzahlen von Ma 3 bis 6", Z. Flugwiss., 13, 7, pp. 237-246, 1965.

Ludwieg, H., "Der Rohrwindkanal", Z. Flugwiss., 3, 7, pp. 206-216, 1955.

Merkli, P. E., "Pressure Recovery in Constant Area Supersonic Diffusers", Yale Univ., Dept. of Eng. & Appl. Sci., Report # 2 and 4 prepared for AFOSR Grant No. 44620-73-C-0032, 1975a.

Merkli, P. E., "Pressure Recovery in Rectangular Adjustable Area Supersonic Diffusers", Yale Univ., Dept. of Eng. & Appl. Sci., Report # 3 prepared for AFOSR Grant No. 44620-73-C-0032, 1975b.

Merkli, P. E., "Pressure Recovery in Rectangular Constant Area Supersonic Diffusers", AIAA J., 14, 2, pp.168-172, 1976.

Merkli, P. E. and Abuaf, N., "The Flow Starting Process of Constant Area Supersonic Diffusers in a Ludwieg Tube", Yale Univ., Dept. of Eng. & Appl. Sci., Report # 5 prepared for AFOSR Grant No. F 44620-73-C-0032, 1976.

Miller, R. H., "Comments of the Tube Wind Tunnel Concept", Aerospace Sciences Lab., Lockheed-Georgia Comp., Res. Mem. ER-9457, 1967.

Wegener, P. P. and Cagliostro, D. J., "Periodic Nozzle Flow with Heat Addition", Comb. Sci. and Tech., 6, pp. 265-277, 1973.

Whitham, G. B., "On the Propagation of Shock Waves through Regions of Nonuniform Area of Flow", J. Fluid Mech., 4, pp. 337-360, 1958.

ACKNOWLEDGEMENT

The author would like to express his thanks to Professors P. P. Wegener and B. J. C. Wu for their cooperation and stimulating discussions. The two-dimensional supersonic nozzle contour was provided by the U.S. Naval Ordnance Laboratory, White Oak, MD.

TABLE I

VARIATION OF THE STARTING TIME, t_{s2}(ms), WITH THE INITIAL PRESSURE RATIO, p_1/p_o, FOR THE NOZZLE EXIT, x = 0 inches, FOR VARIOUS DIFFUSERS. UPSTREAM DIAPHRAGM LOCATION.

NOZZLE	$t_{s2} = 31.7\ (p_1/p_o) + 0.06$	$0<p_1/p_o<0.1$
NOZZLE + 3 inch DIFFUSER	$t_{s2} = 17.87\ (p_1/p_o) + 0.63$	$0<p_1/p_o<0.13$
NOZZLE + 6 inch DIFFUSER	$t_{s2} = 23.3\ (p_1/p_o) + 0.50$	$0<p_1/p_o<0.15$
NOZZLE + 9 inch DIFFUSER	$t_{s2} = 28\ (p_1/p_o) + 0.32$	$0<p_1/p_o<0.18$
NOZZLE + 12 inch DIFFUSER	$t_{s2} = 38.16\ (p_1/p_o) - 0.25$	$0<p_1/p_o<0.20$

TABLE II

VARIATION OF THE STARTING TIME, t_{s2}(ms), WITH THE INITIAL PRESSURE RATIO, p_1/p_o, FOR THE DIFFUSER EXIT FOR VARIOUS DIFFUSERS. UPSTREAM DIAPHRAGM LOCATION.

NOZZLE (at x = 0 inches)	$t_{s2} = 31.7\ (p_1/p_o) + 0.06$	$0<p_1/p_o<0.1$
NOZZLE + 3 inch DIFFUSER (at x = 3 inches)	$t_{s2} = 28.76\ (p_1/p_o) + 0.47$	$0<p_1/p_o<0.1$
NOZZLE + 6 inch DIFFUSER (at x = 6 inches)	$t_{s2} = 38.66\ (p_1/p_o) + 0.26$	$0<p_1/p_o<0.1$
NOZZLE + 9 inch DIFFUSER (at x = 9 inches)	$t_{s2} = 52.97\ (p_1/p_o) + 0.23$	$0<p_1/p_o<0.1$
NOZZLE + 12 inch DIFFUSER (at x = 12 inches)	$t_{s2} = 54.01\ (p_1/p_o) + 0.51$	$0<p_1/p_o<0.1$

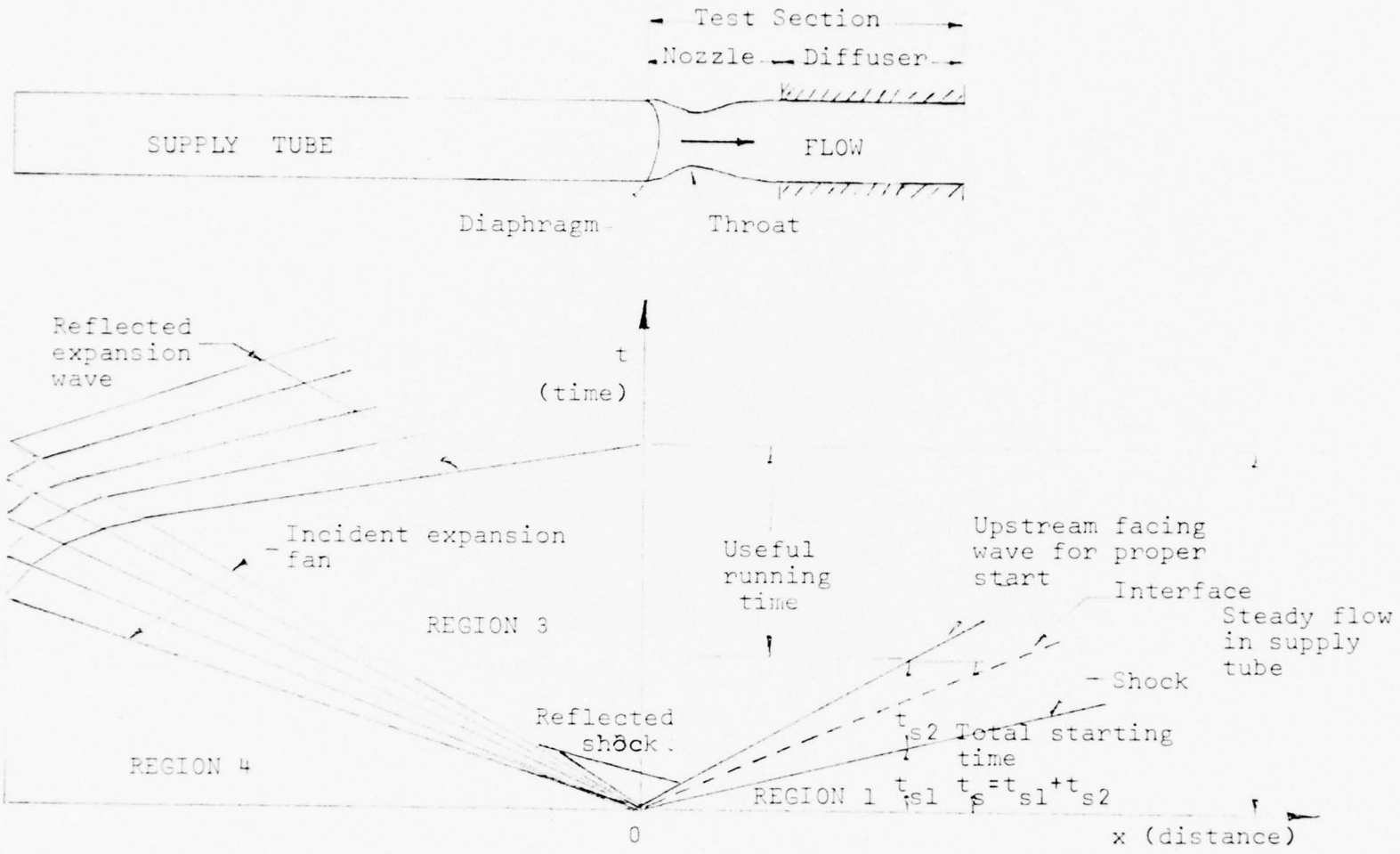

Figure 1. Approximate wave diagram for the flow in a Ludwieg tube with an upstream diaphragm location (Hottner, 1965; Davis and Gwin, 1967).

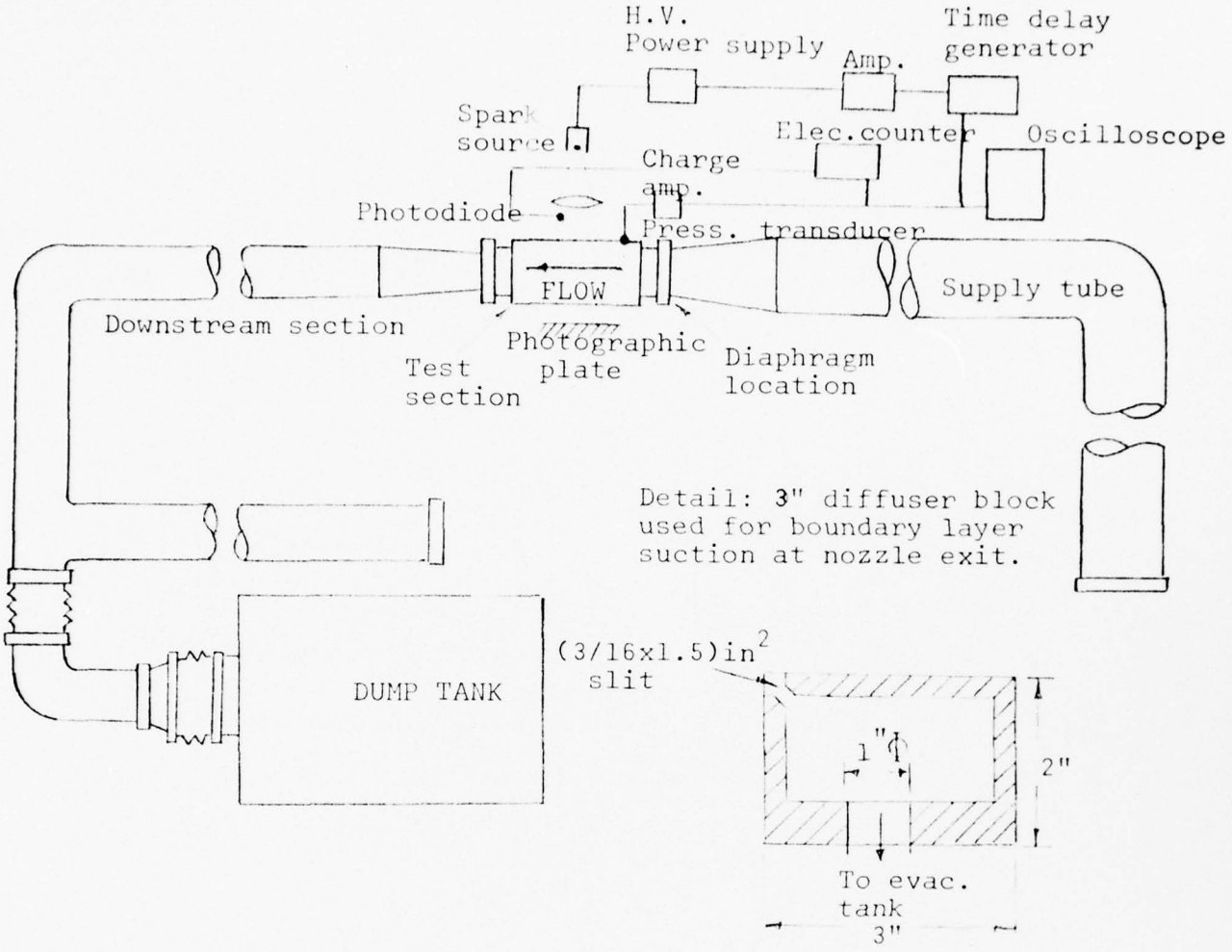

Figure 2a. The experimental set-up.

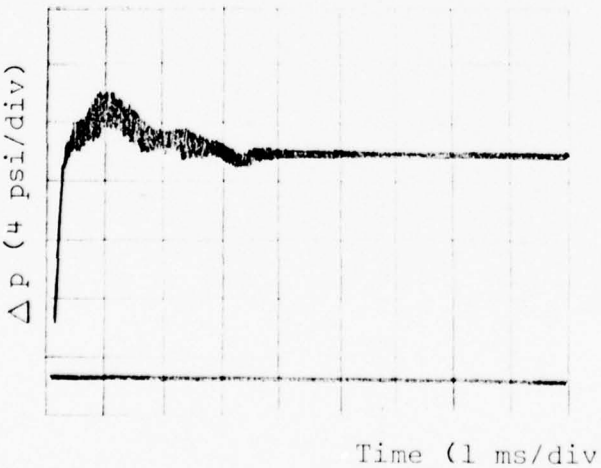

9" diffuser. Upstream diaphragm.
p_o=966 torr, T_o=293K, p_1=48 torr.
x^o= -10 in.

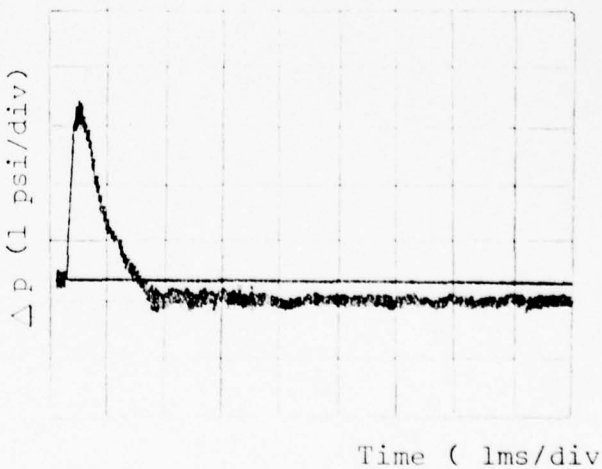

9" diffuser. Upstream diaphragm.
p_o=966 torr, T_o=293K, p_1=48 torr.
x^o= 0 in.(nozzle exit).

Figure 2b. Typical oscillograms.

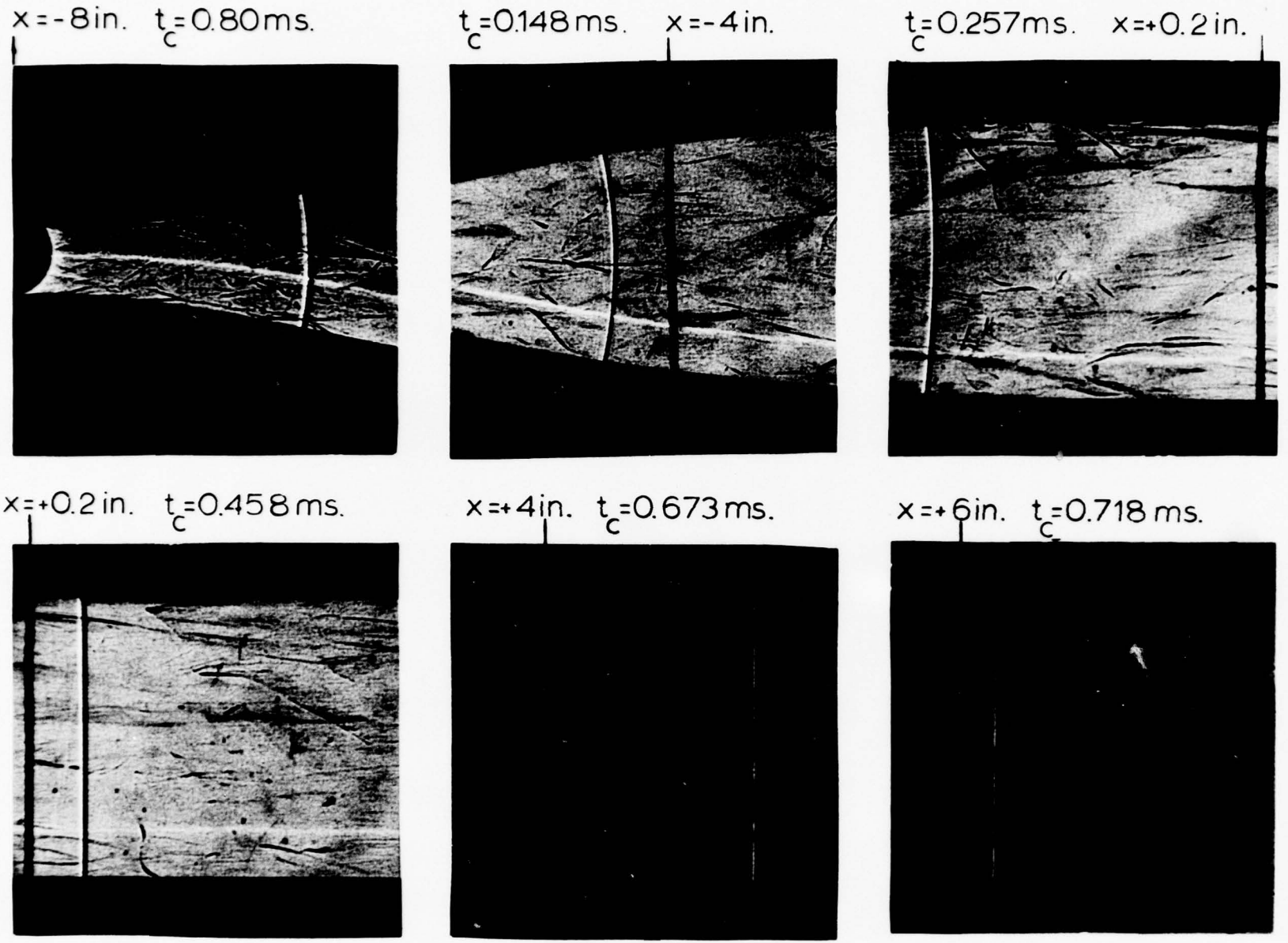

Figure 3. Typical shadowgraph pictures of the shock wave travelling through the nozzle-6 in. diffuser section. Upstream diaphragm location. p_o=966 torr (p_4=1000 torr), T_o=293 K, p_1=150 torr. The time, t_c, of the counter reading starts with the arrival of the shock to the nozzle throat.

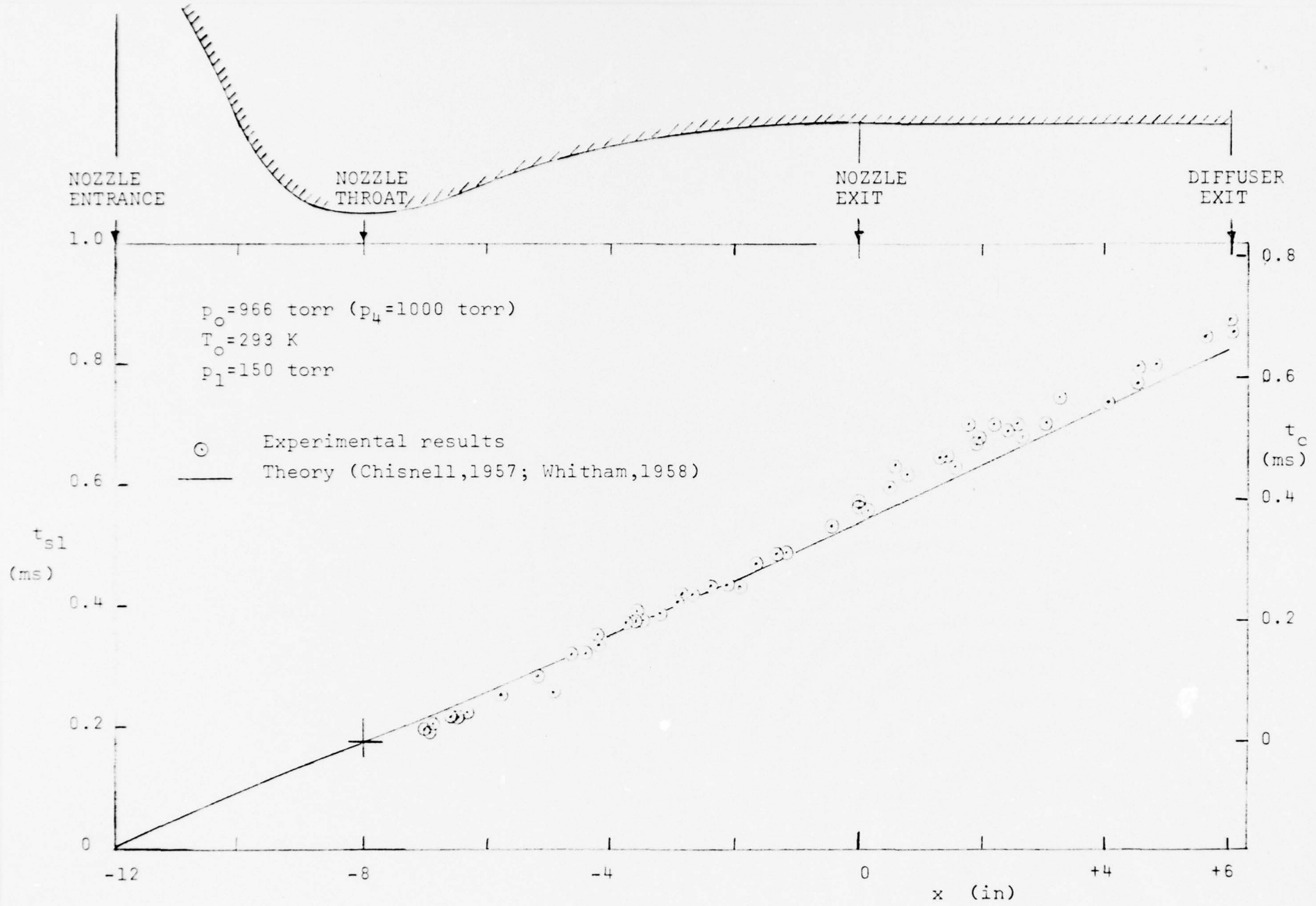

Figure 4. x-t diagram for the shock wave traveling through the nozzle and 6in. diffuser assembly. Upstream diaphragm location. Comparison of experimental results with theoretical calculations.

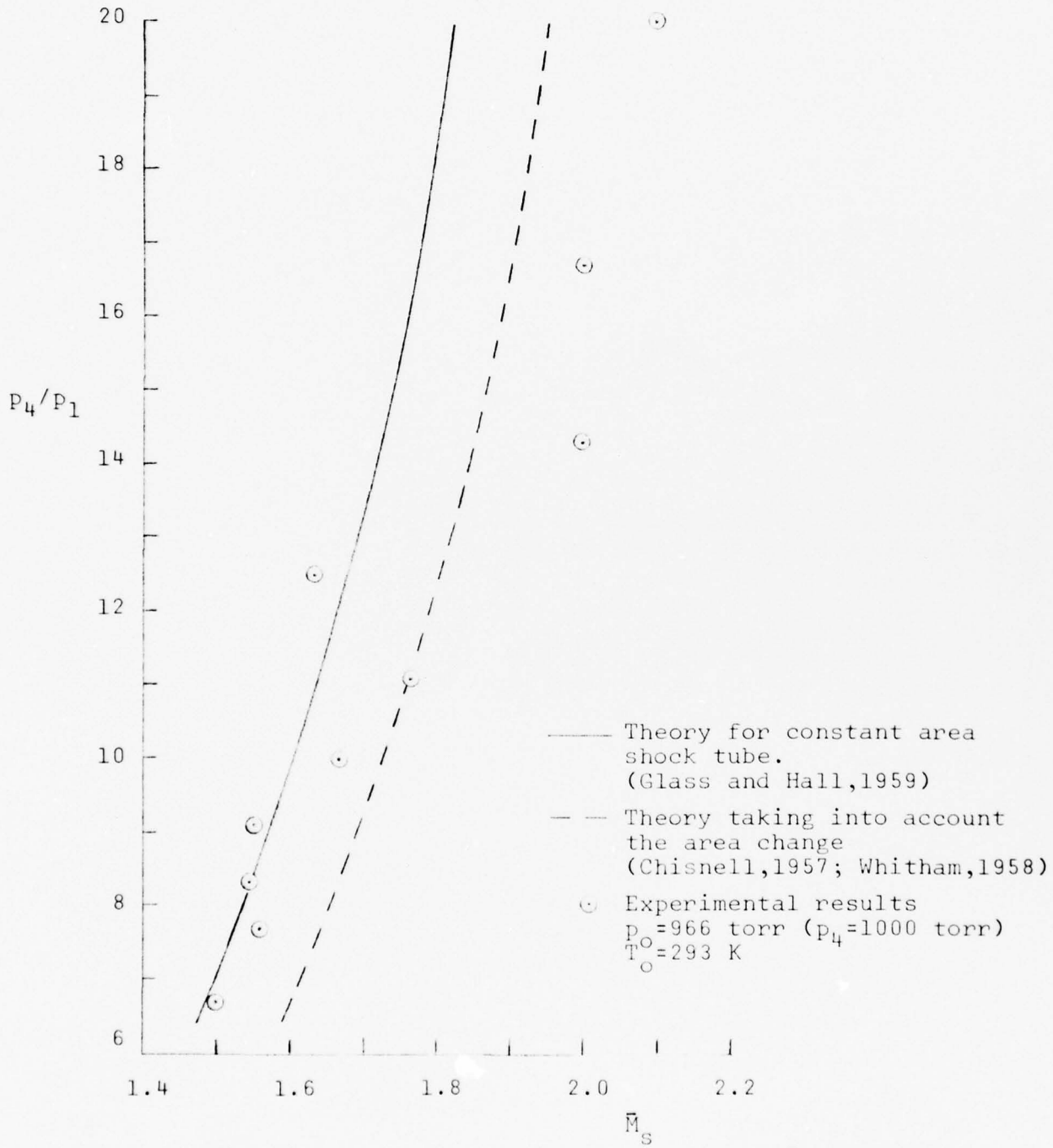

Figure 5. Variation of average shock Mach number, $\bar{M}_s$, as a function of initial pressure ratio, p_4/p_1. Upstream diaphragm location. Comparison of experiments (6 in. diffuser) with theoretical calculations.

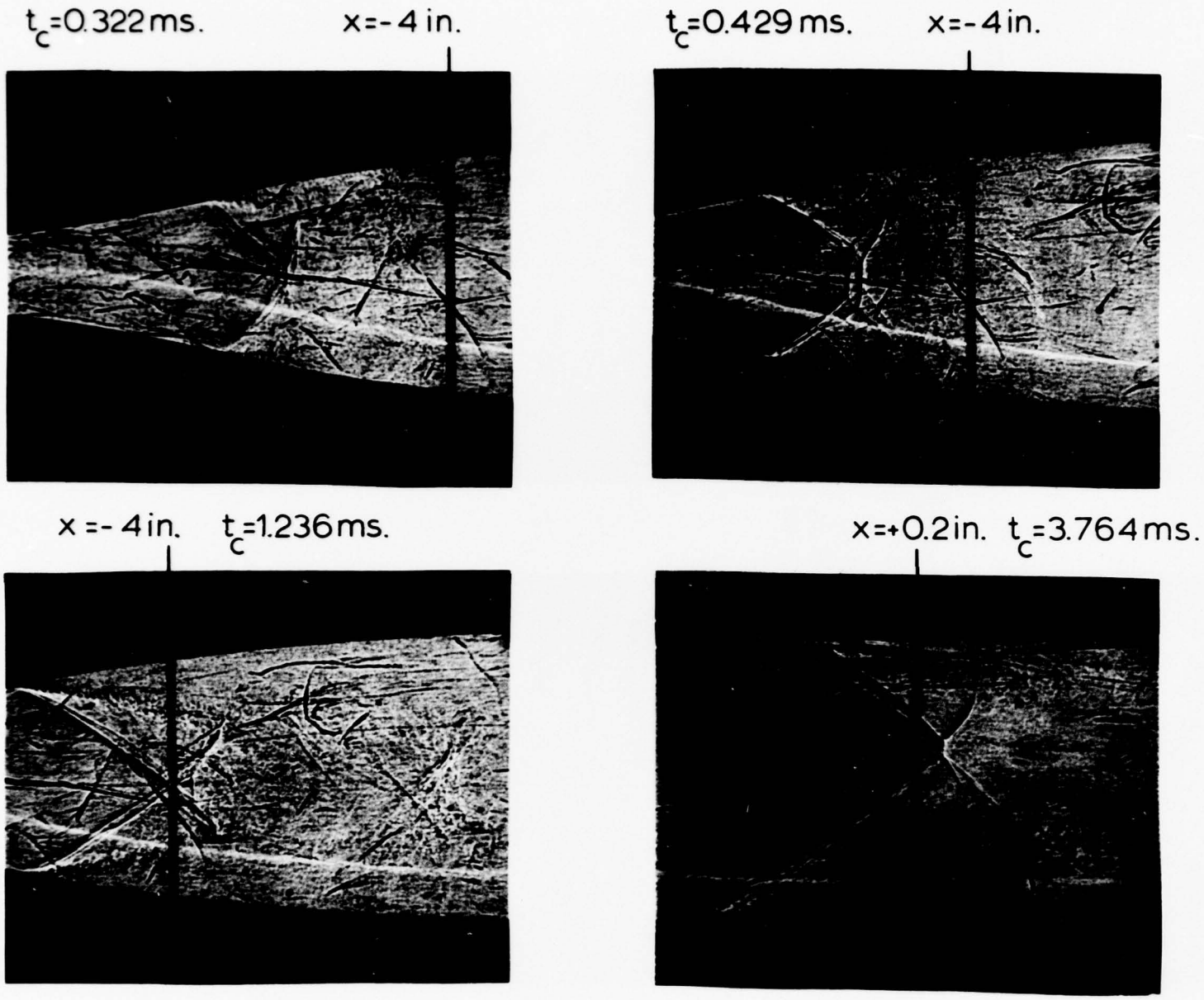

Figure 6. Typical shadowgraph pictures of the upstream facing wave. Upstream diaphragm location. 6 in. diffuser. p_o=966 torr, T_o=293 K, p_1=150 torr. The time reading, t_c, of the counter starts with the arrival of the shock wave to the nozzle throat.

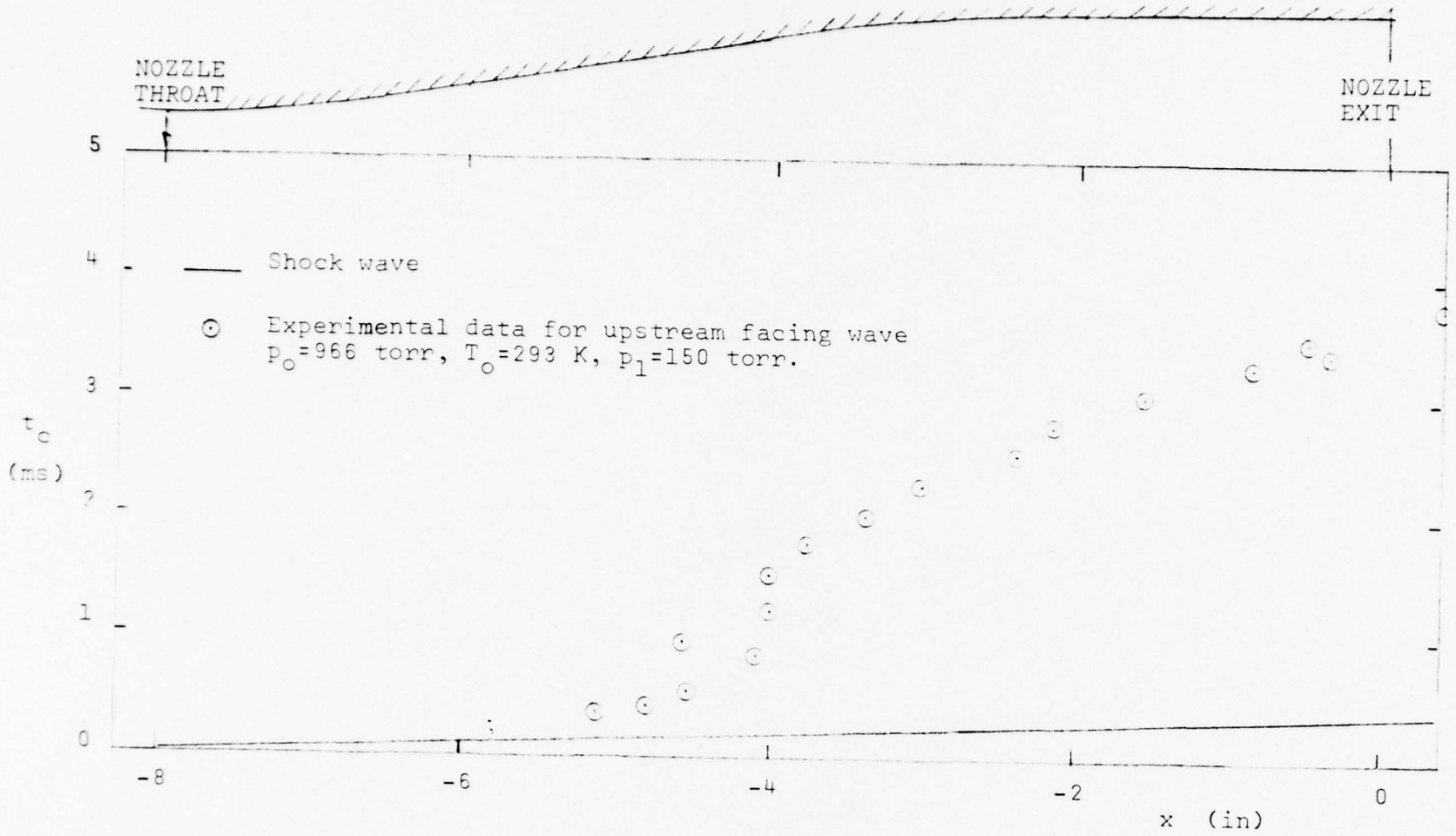

Figure 7. x-t diagram for shock wave and upstream facing wave. Upstream diaphragm location. 6 in diffuser.

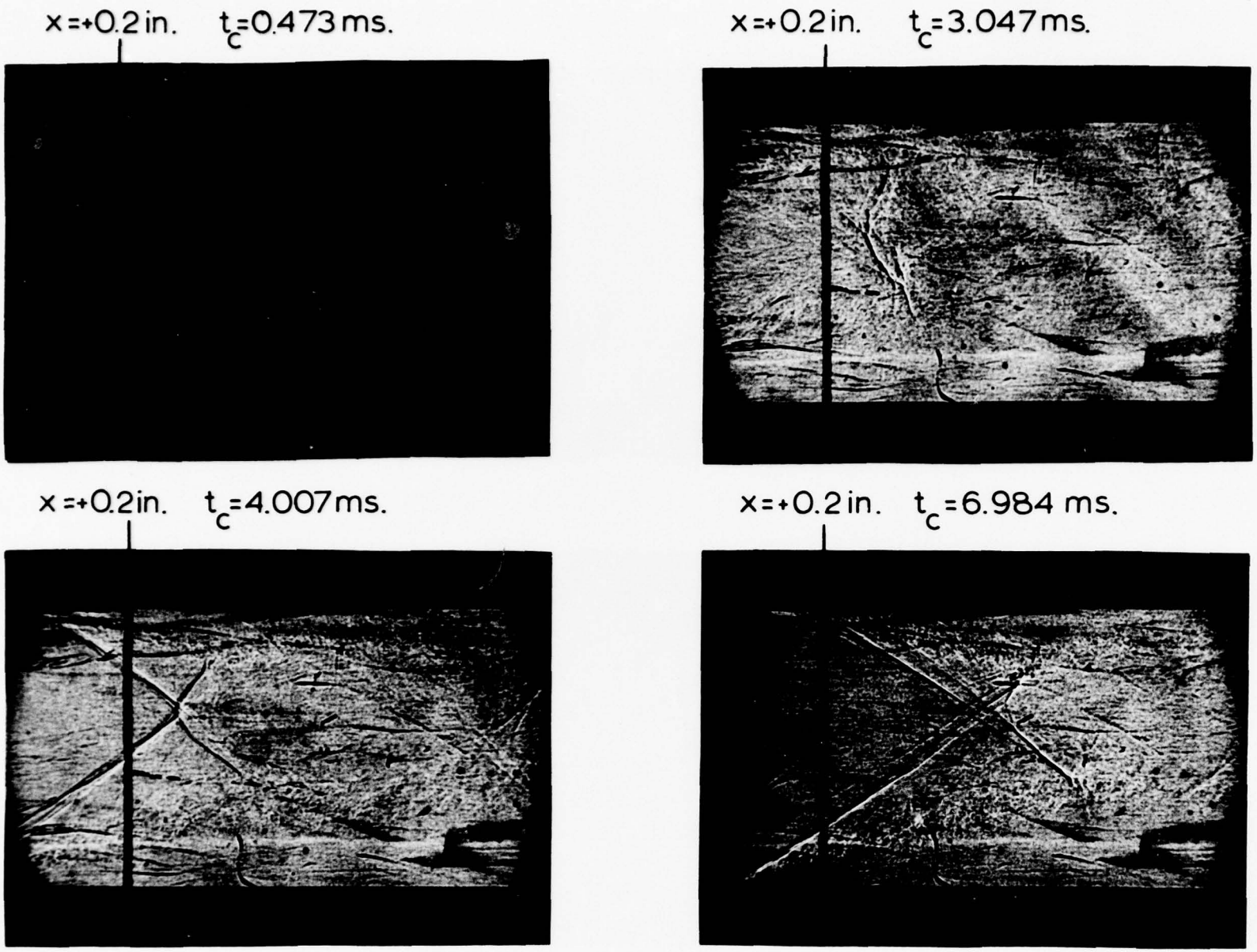

Figure 8. Shadowgraphs of the flow field at the nozzle exit as a function of time. Upstream diaphragm location. 6 in. diffuser. p_o=966 torr, T_o=293 K, p_1=150 torr. The time, t_c, of the counter readings starts with the arrival of the shock to the nozzle throat.

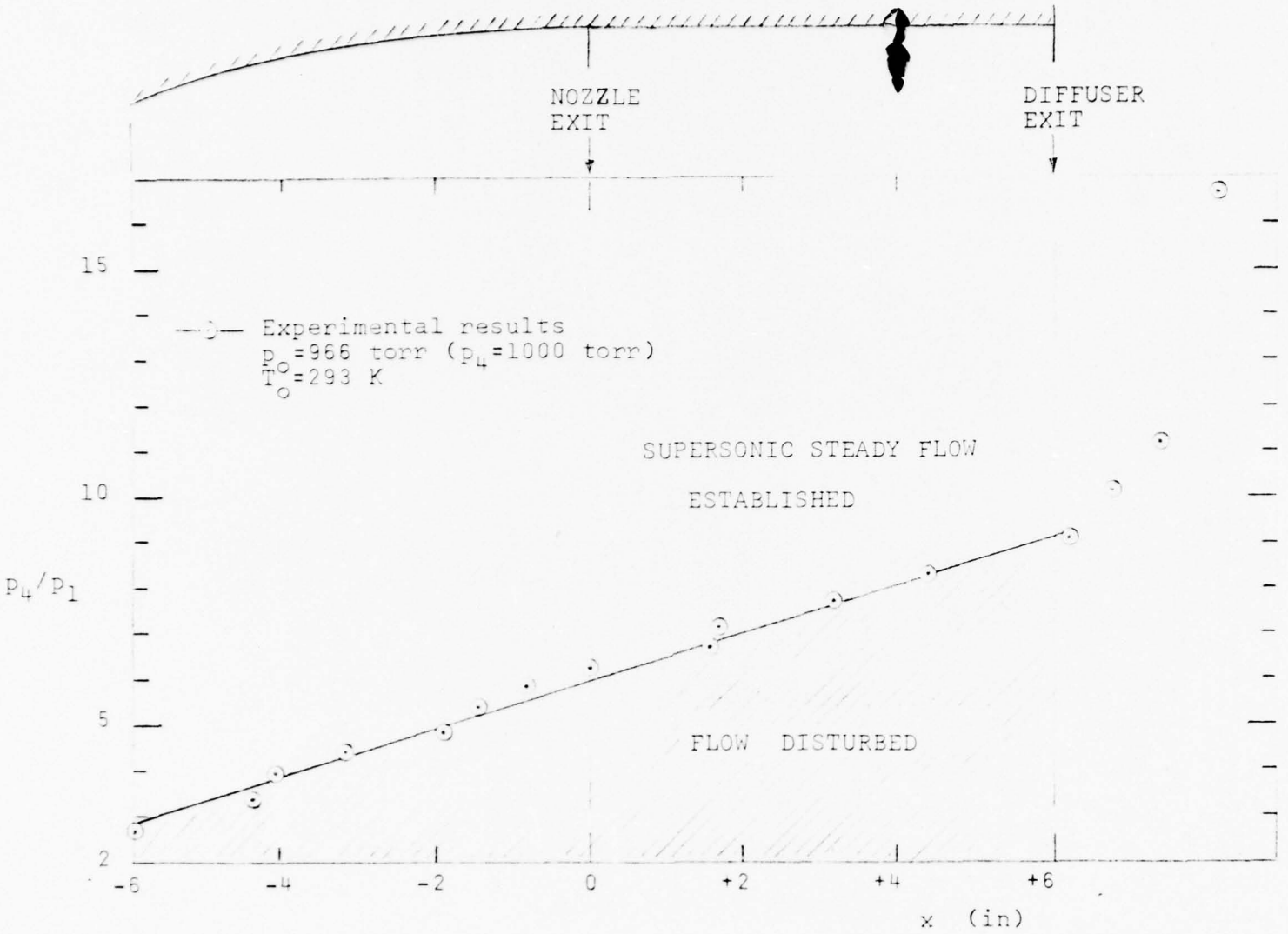

Figure 9. Location of the upstream facing shock as a function of initial pressure ratio, p_4/p_1. Upstream diaphragm location. 6 in. diffuser. Time (7 ms) is long enough to establish steady flow conditions whenever possible.

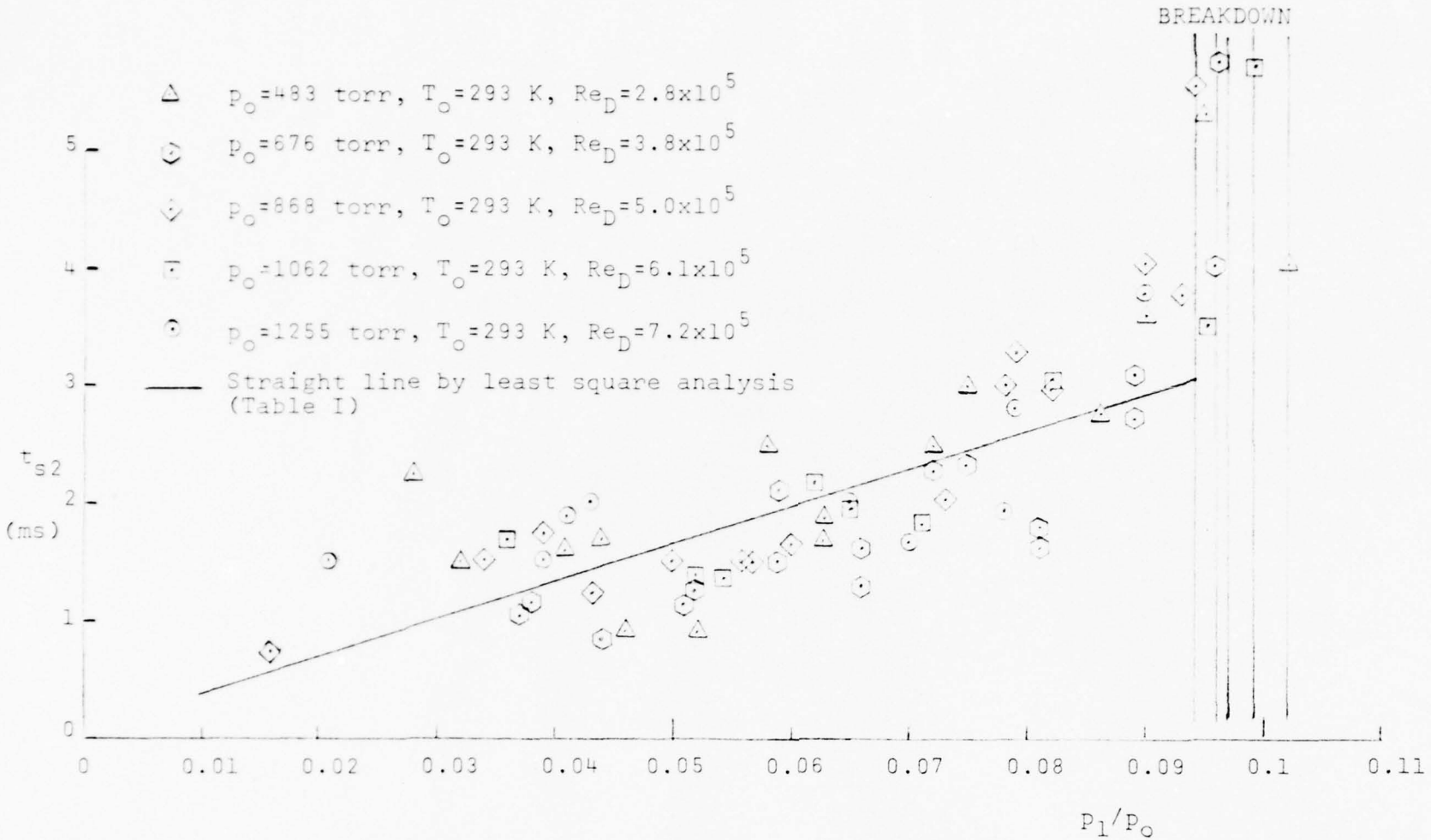

Figure 10. Starting times for the flow, t_{s2}, at the nozzle exit as a function of initial pressure ratio, p_1/p_o, for the case of the nozzle without a diffuser. Upstream diaphragm location. Nozzle entrance at 1.81 in. from diaphragm.

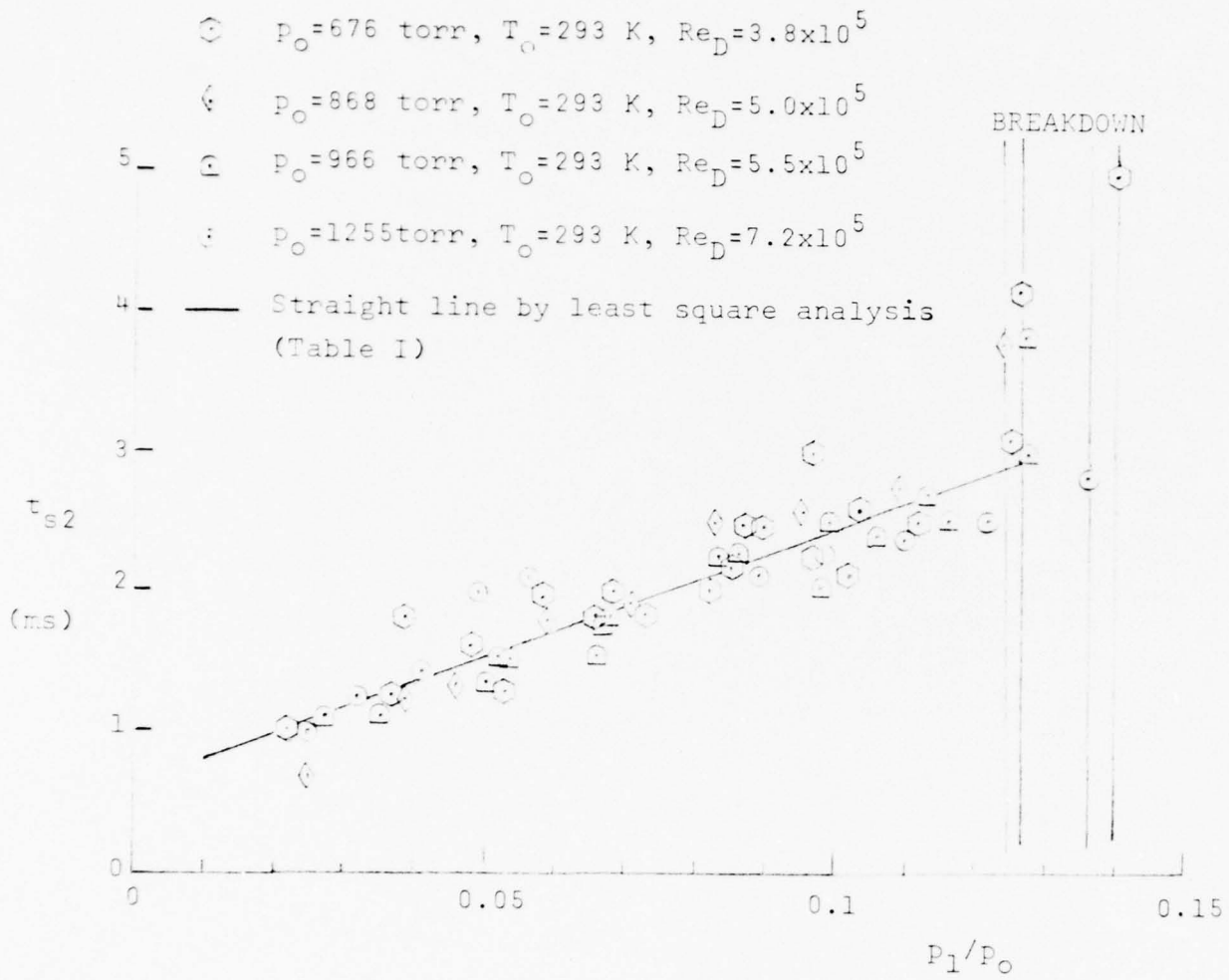

Figure 11. Starting times for the flow, t_{s2}, at nozzle exit as a function of initial pressure ratio, p_1/p_o. Diffuser length, L/D= 1.5. Upstream diaphragm location. Nozzle entrance at 1.81 in. from diaphragm.

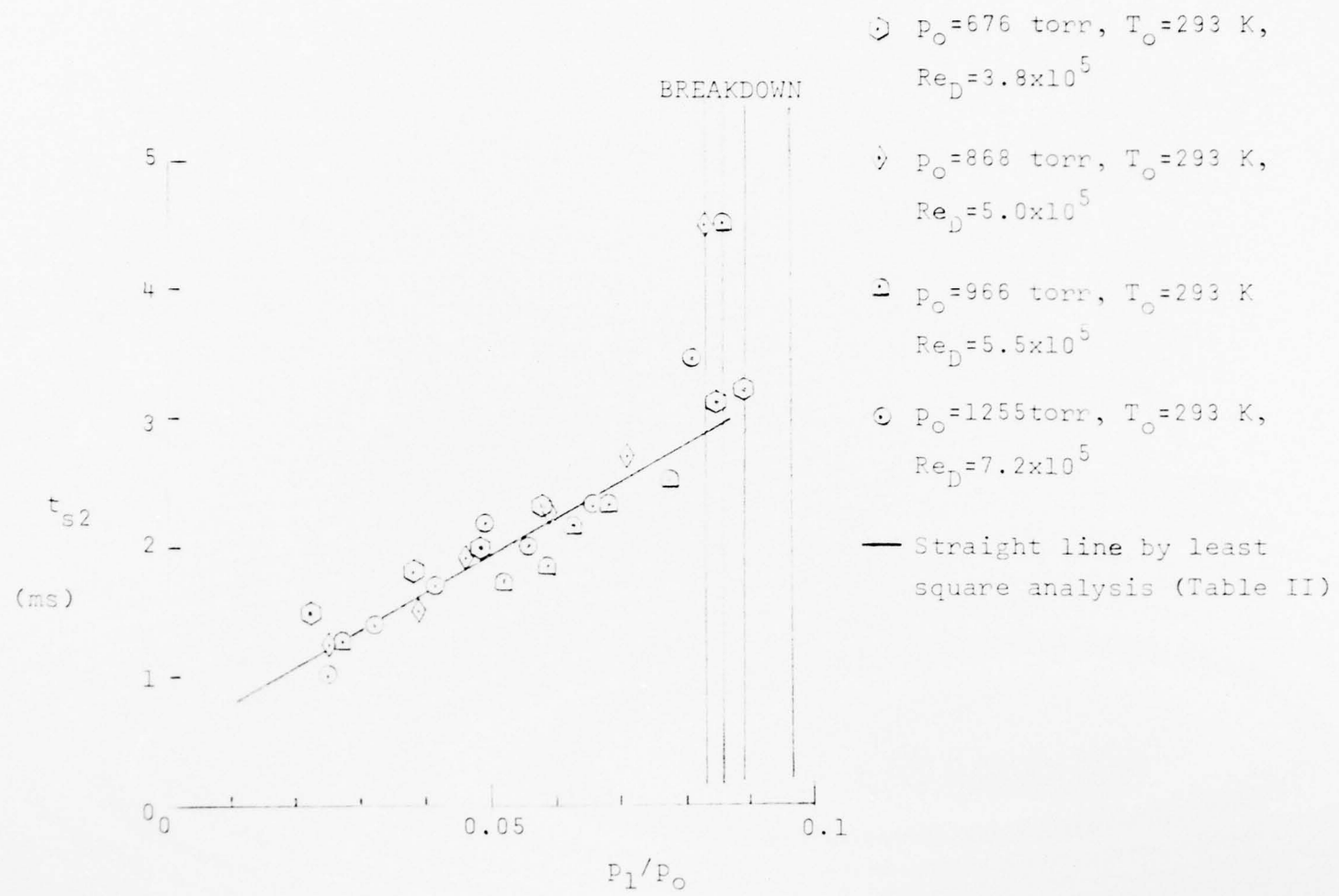

Figure 12. Starting times for the flow, t_{s2}, at the diffuser exit as a function of initial pressure ratio, p_1/p_o. Diffuser length, L/D = 1.5. Upstream diaphragm location. Nozzle entrance at 1.81 in. from diaphragm.

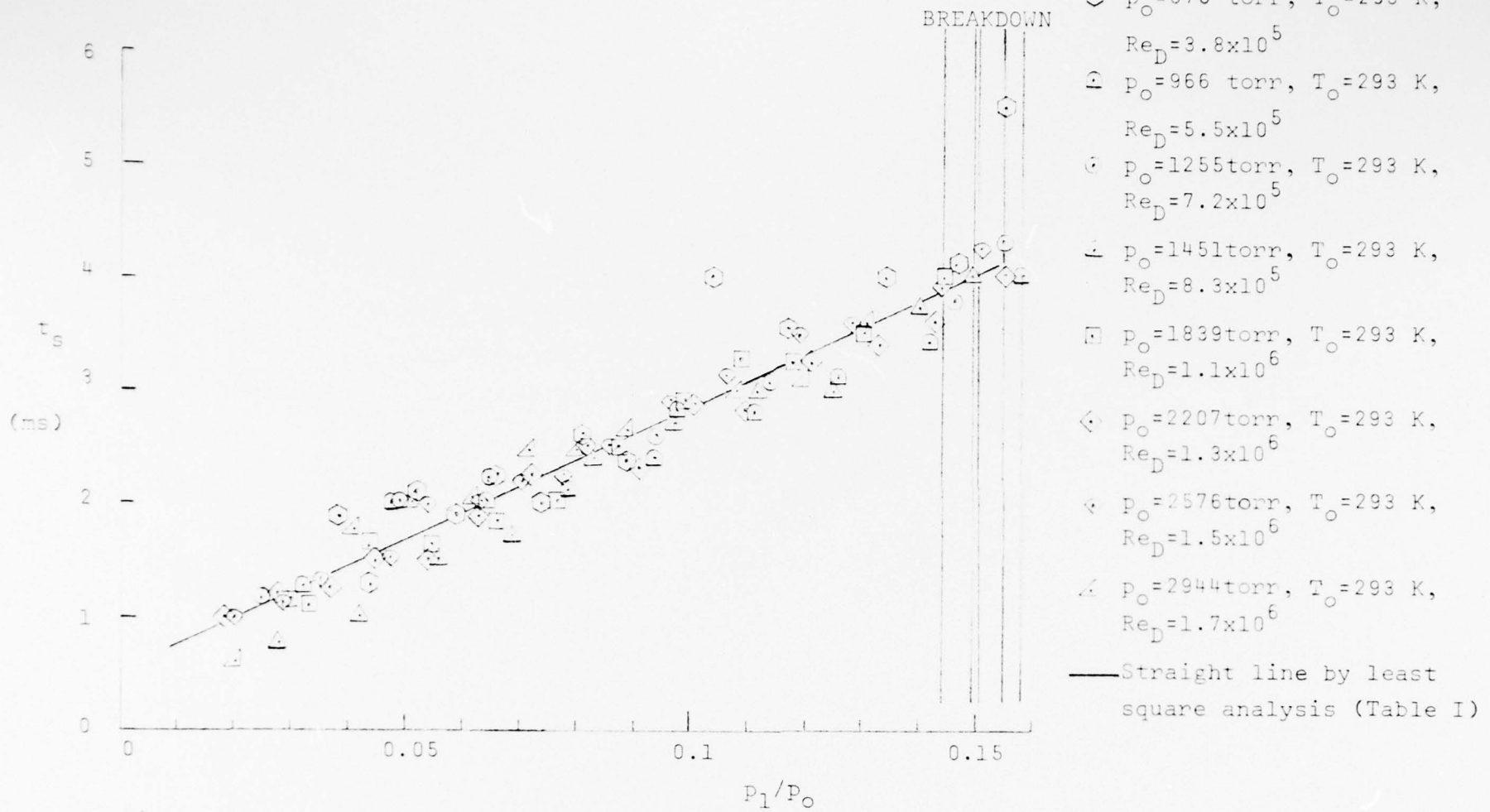

Figure 13. Starting times for flow, t_{s2}, at the nozzle exit as a function of initial pressure ratio, p_1/p_o. Diffuser length, L/D = 3. Upstream diaphragm location. Nozzle at 1.81 in. from diaphragm.

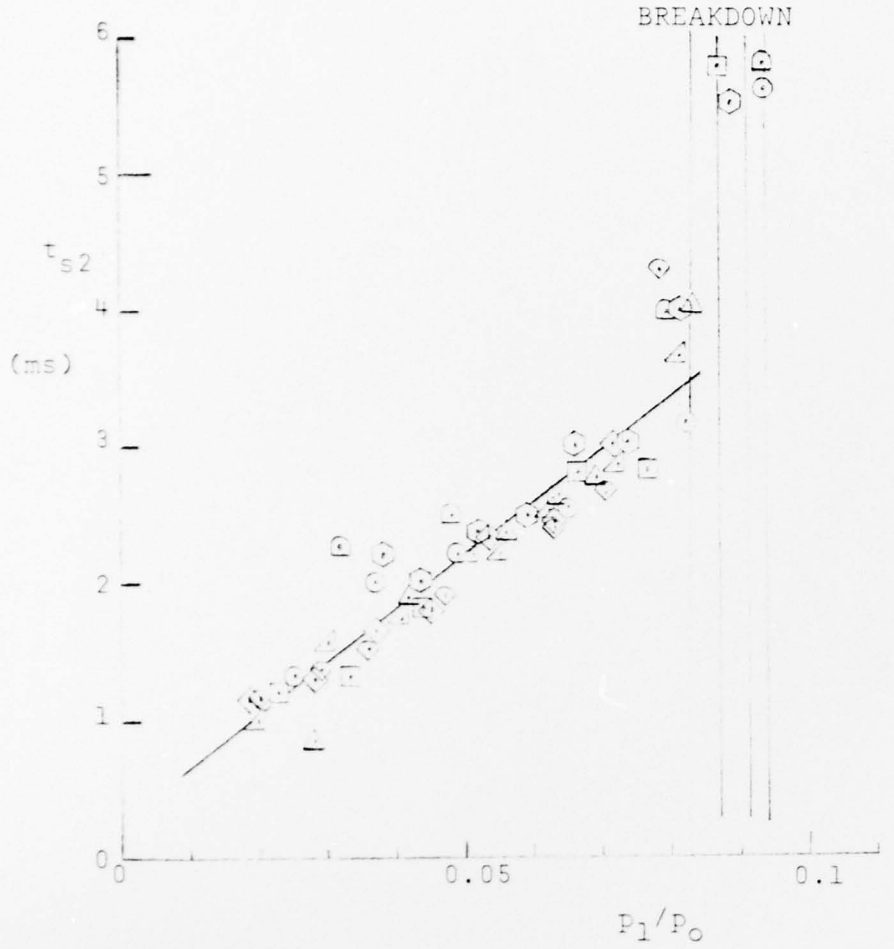

p_o=676 torr, T_o=293 K, $Re_D=3.8\times10^5$

p_o=966 torr, T_o=293 K, $Re_D=5.5\times10^5$

p_o=1255torr, T_o=293 K, $Re_D=7.2\times10^5$

p_o=1451torr, T_o=293 K, $Re_D=8.3\times10^5$

p_o=1839torr, T_o=293 K, $Re_D=1.1\times10^6$

p_o=2207torr, T_o=293 K, $Re_D=1.3\times10^6$

p_o=2576torr, T_o=293 K, $Re_D=1.5\times10^6$

p_o=2944torr, T_o=293 K, $Re_D=1.7\times10^6$

——Straight line by least square analysis (Table II)

Figure 14. Starting times for flow, t_{s2}, at the diffuser exit as a function of initial pressure ratio, p_1/p_o. Diffuser length, L/D= 3. Upstream diaphragm location. Nozzle at 1.81 in. from diaphragm.

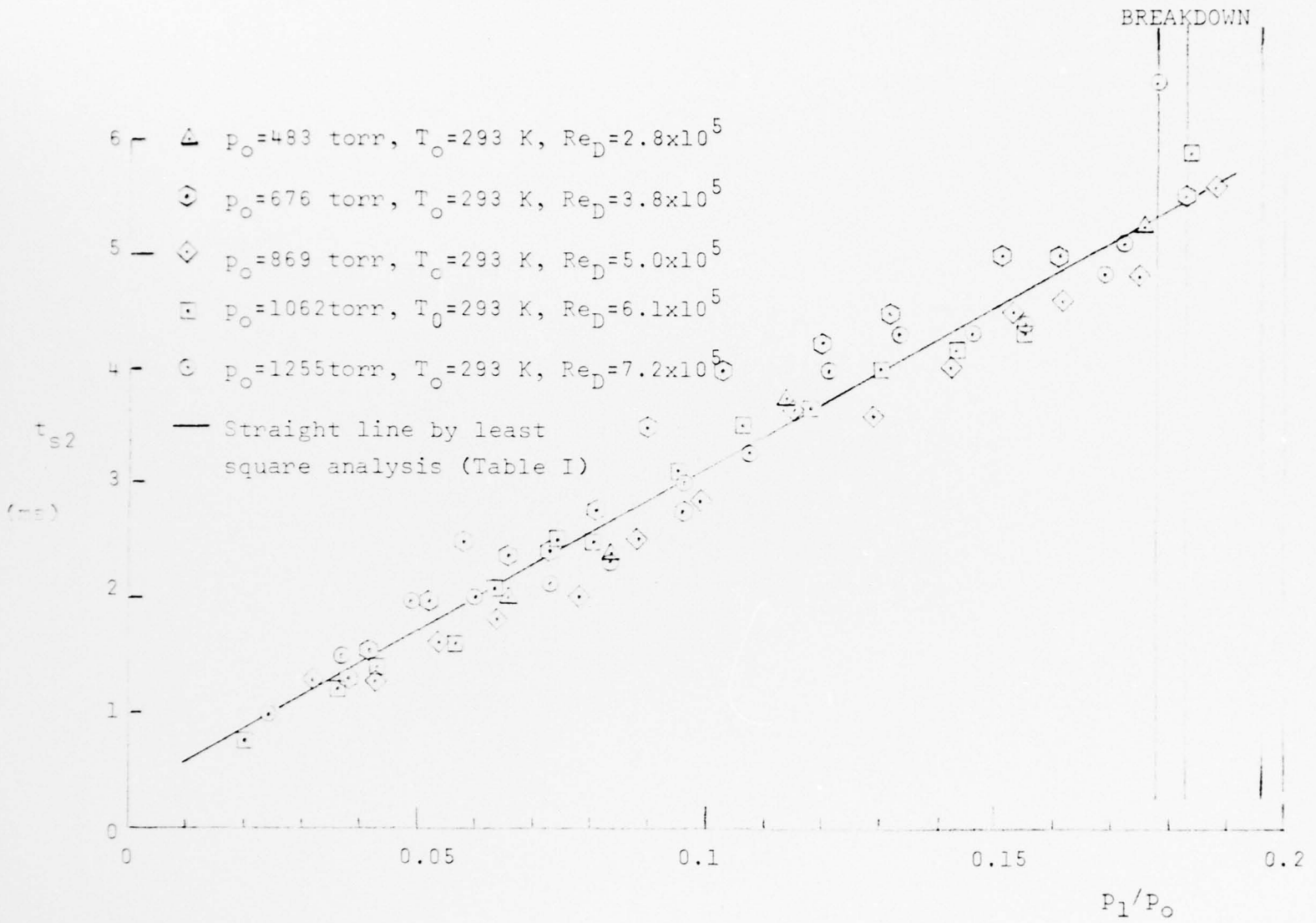

Figure 15. Starting times for flow, t_{s2}, at the nozzle exit as a function of initial pressure ratio, p_1/p_o. Diffuser length, L/D = 4.5. Upstream diaphragm location. Nozzle entrance at 1.81 in. from diaphragm.

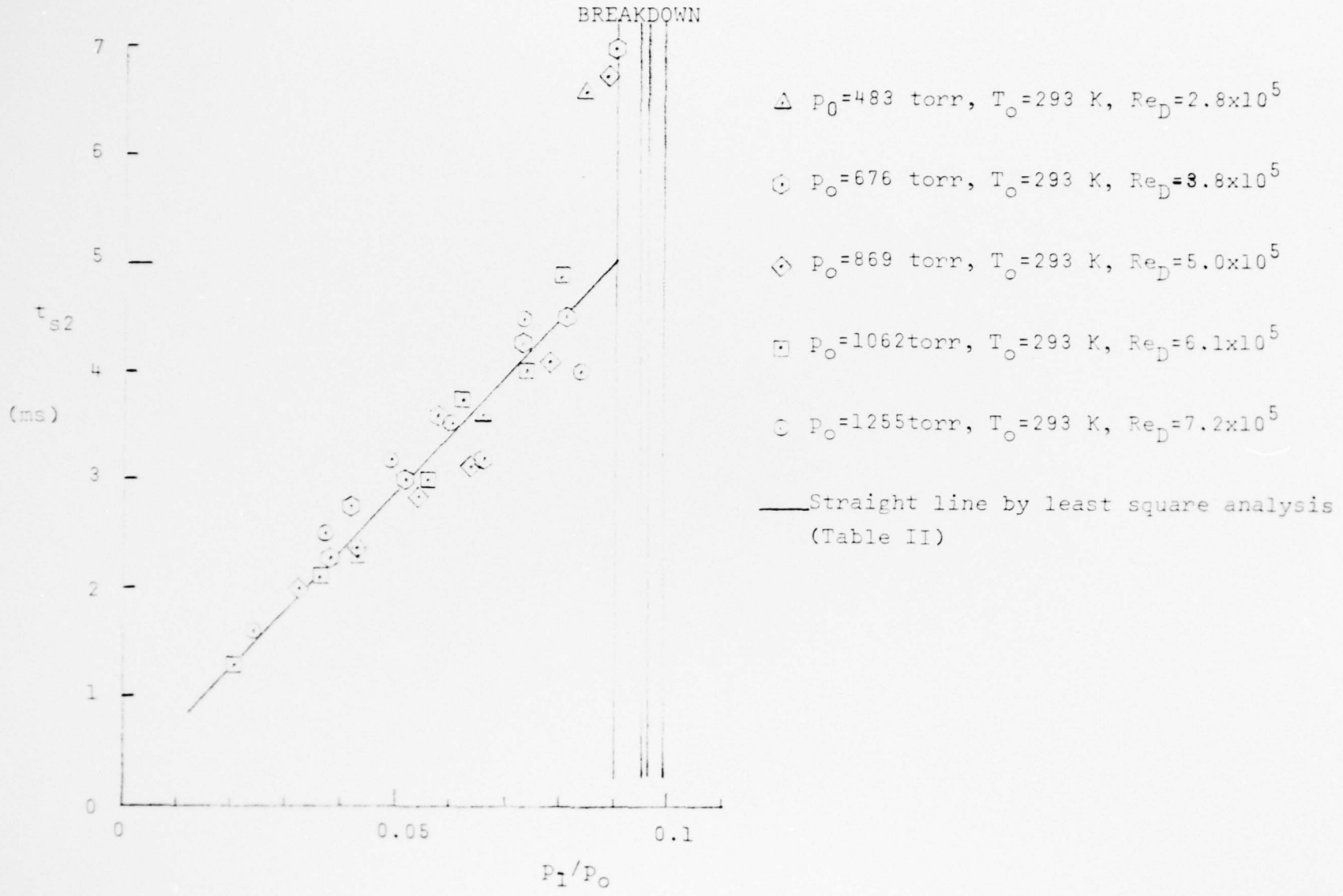

Figure 16. Starting times for the flow, t_{s2}, at the diffuser exit as a function of initial pressure ratio, P_1/P_o. Diffuse-r length, $L/D \cong 4.5$ Upstream diaphragm location.

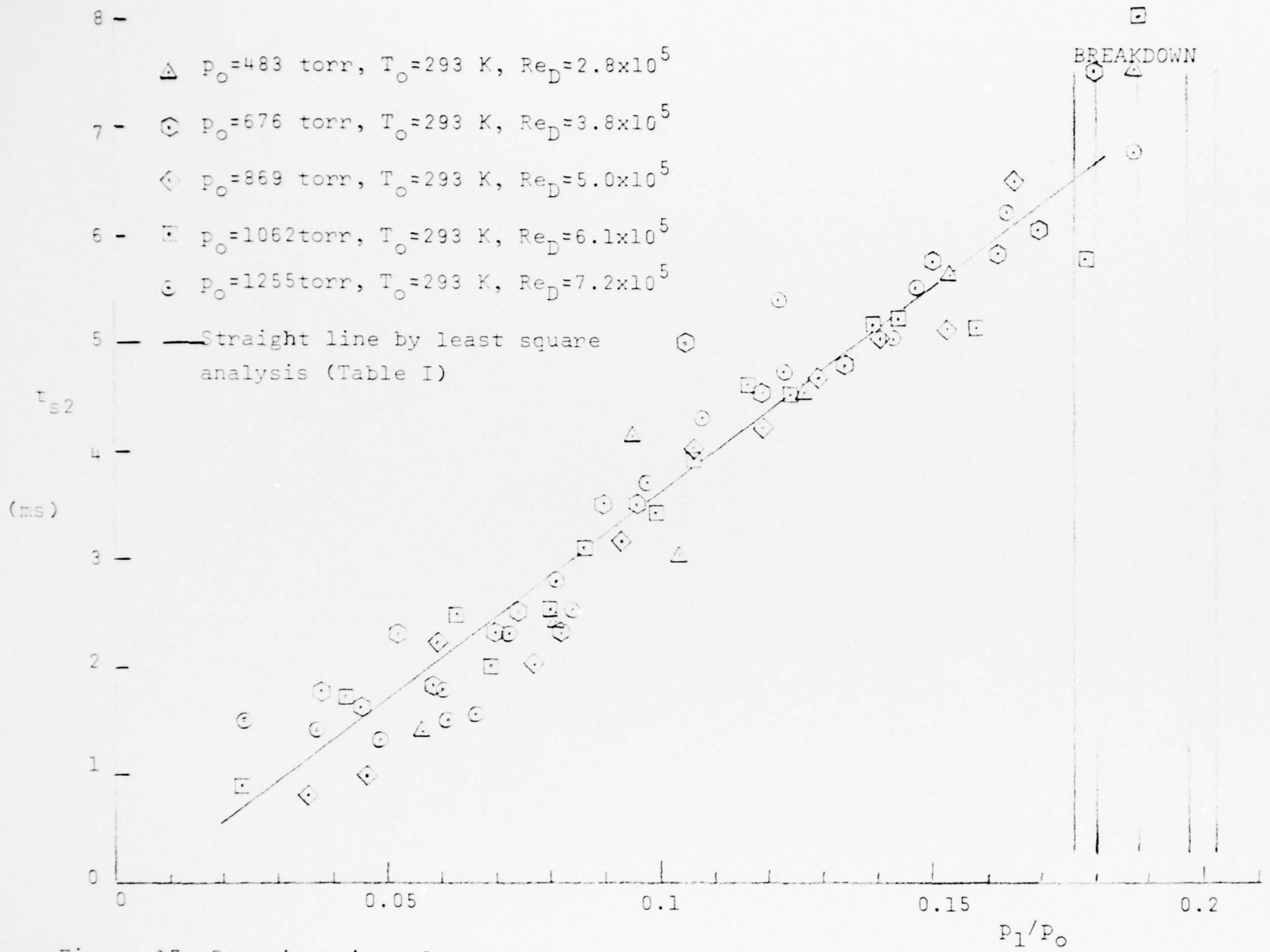

Figure 17. Starting times for the flow, t_{s2}, at the nozzle exit as a function of initial pressure ratio, p_1/p_o. Diffuser length, L/D= 6. Upstream diaphragm location. Nozzle entrance at 1.81 in.from diaphragm.

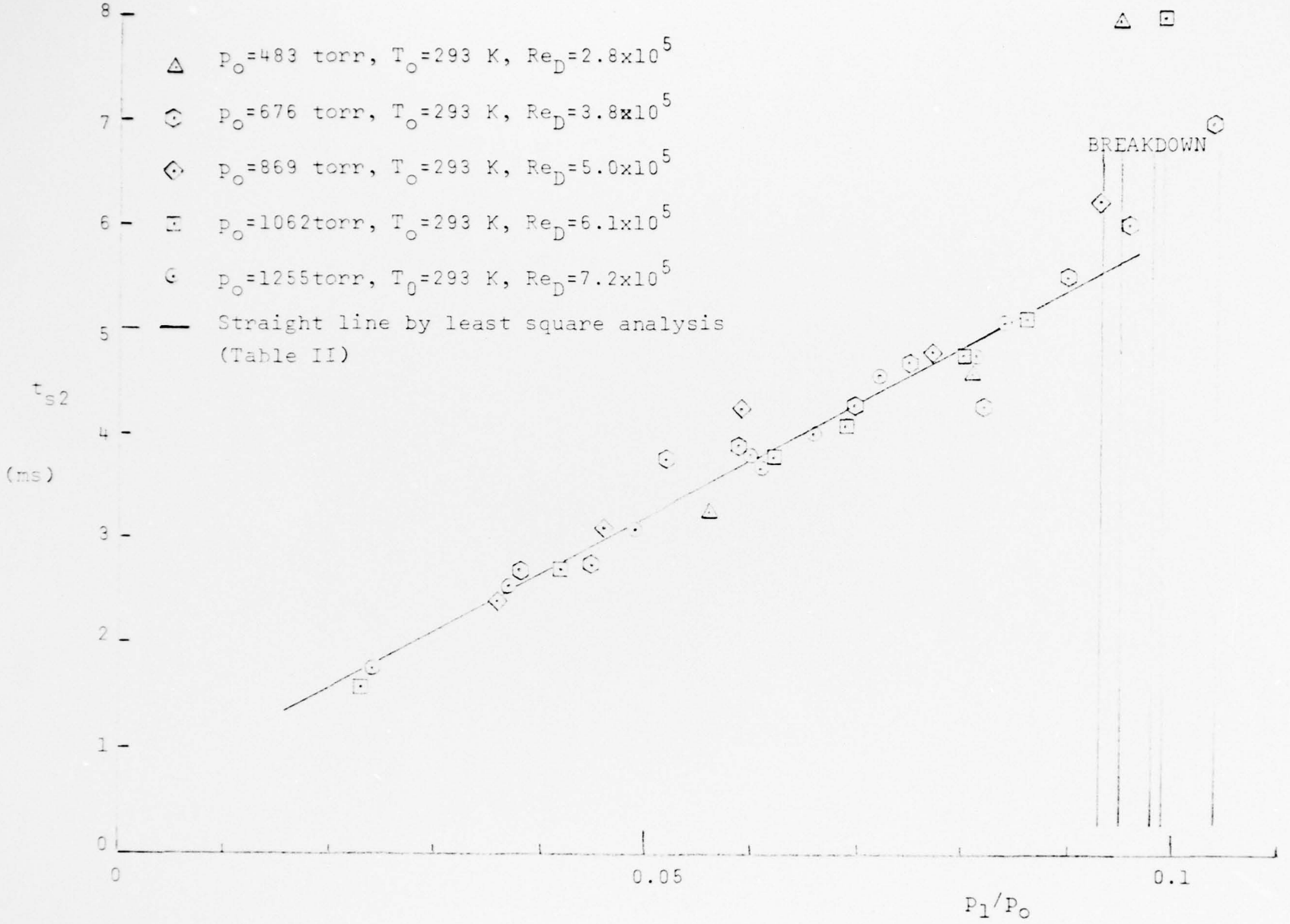

Figure 18. Starting times for the flow, t_{s2}, at the diffuser exit as a function of initial pressure ratio, p_1/p_o. Diffuser length, L/D = 6. Upstream diaphragm location. Nozzle entrance at 1.81 in. from diaphragm.

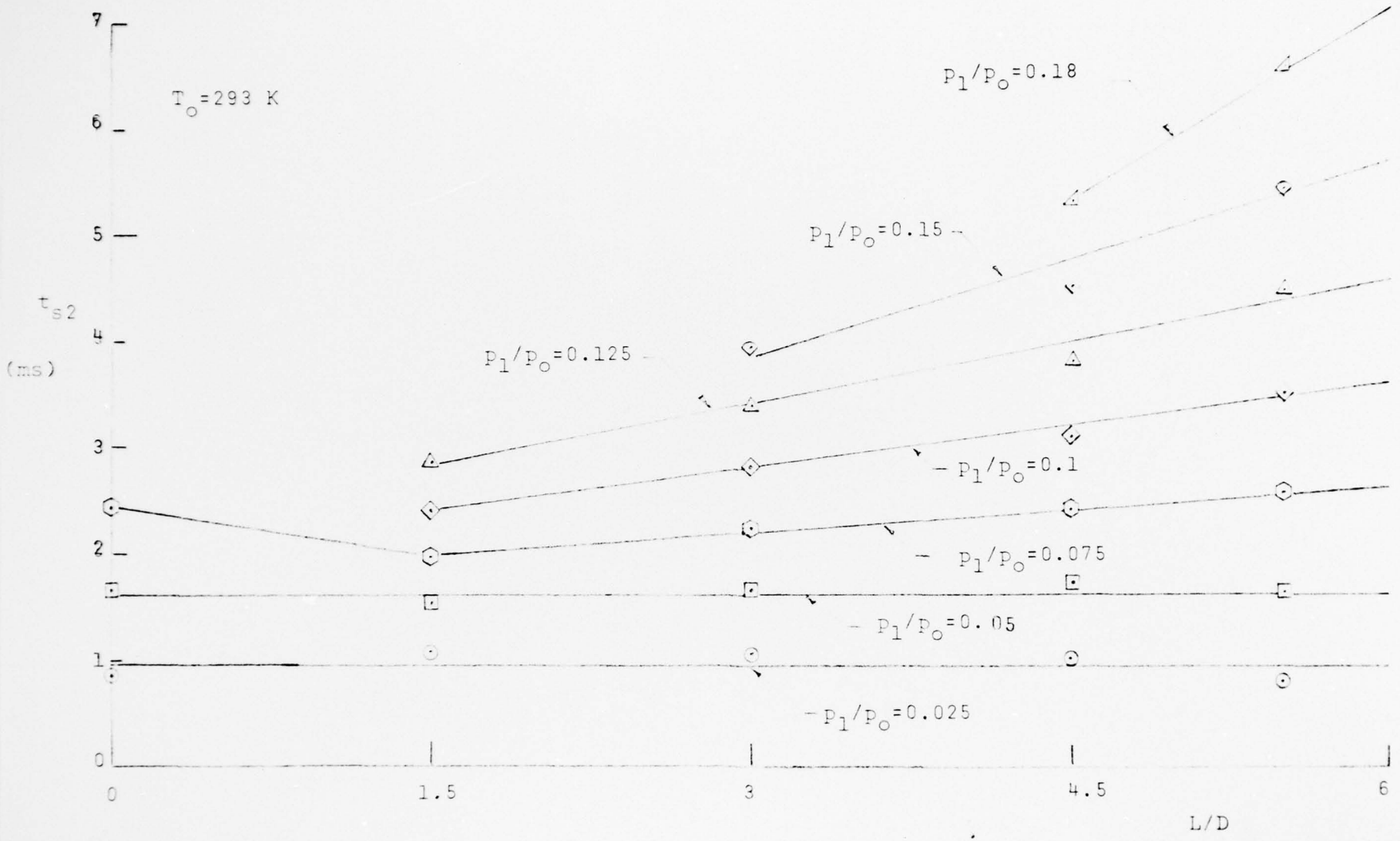

Figure 19. Starting times for the flow, t_{s2}, at the nozzle exit as a function of dimensionless diffuser length, L/D, for various initial pressure ratios, p_1/p_o. Upstream diaphragm location. Nozzle entrance at 1.81 in. from diaphragm.

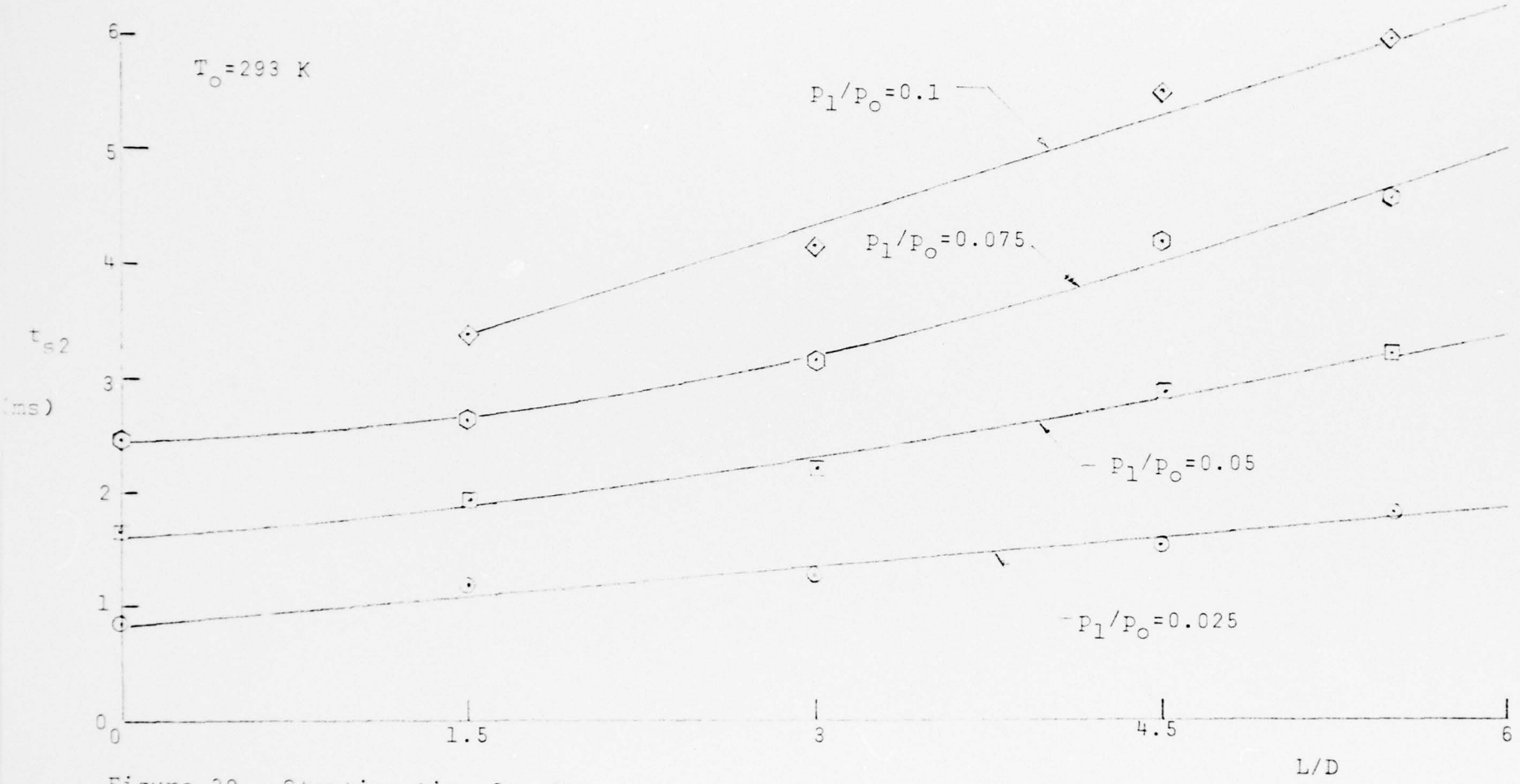

Figure 20. Starting time for flow, t_{s2}, at diffuser exit as a function of dimensionless diffuser length, L/D, for various initial pressure ratios, p_1/p_o. Upstream diaphragm location. Nozzle entrance at 1.81 in. from diaphragm.

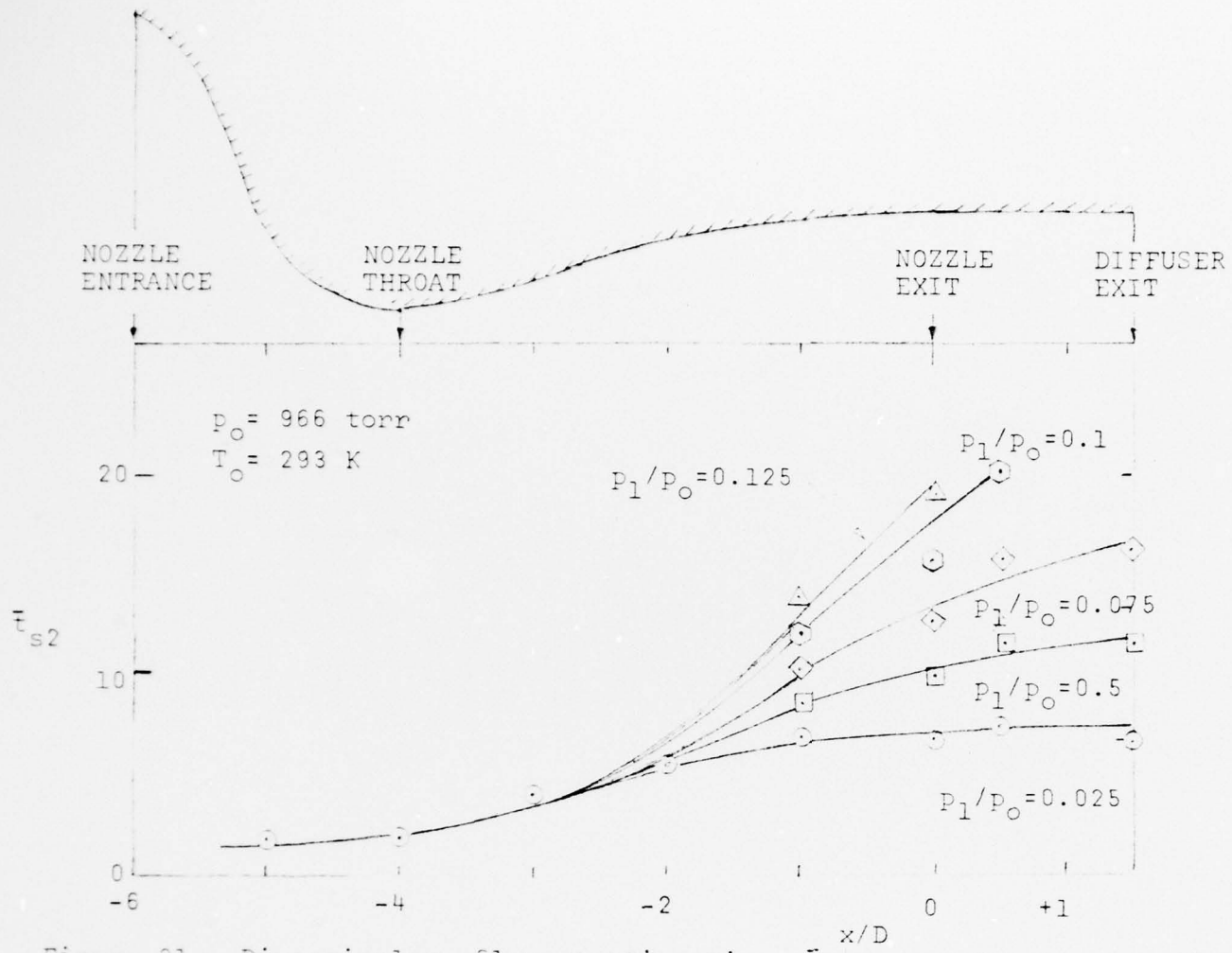

Figure 21. Dimensionless flow starting time, $\bar{t}_{s2}$, as a function of dimensionless axial distance, x/D, for various values of initial pressure ratio, p_1/p_o. Diffuser length L/D = 1.5. Upstream diaphragm location. Nozzle entrance at 1.81 in. from diaphragm.

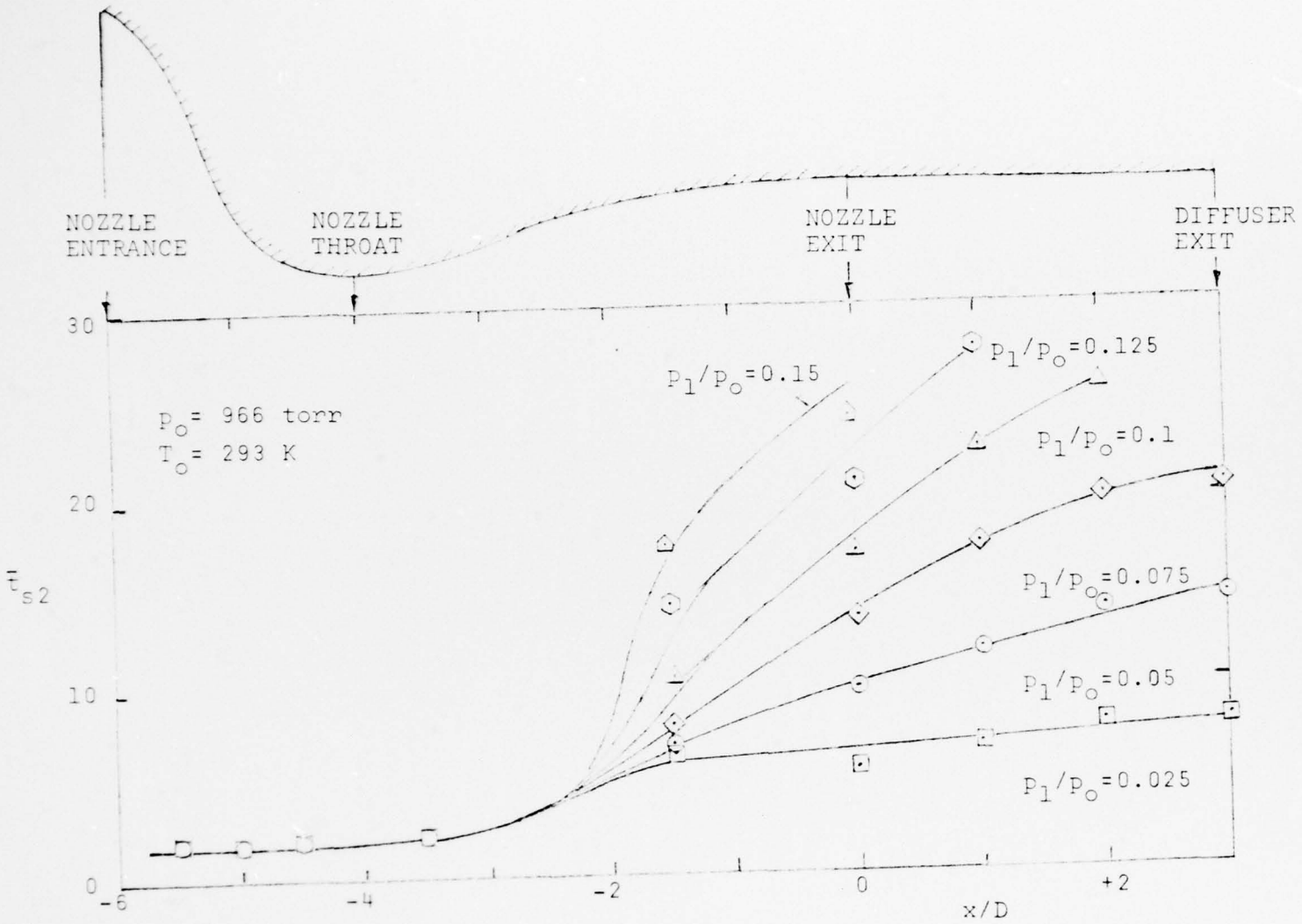

Figure 22. Dimensionless flow starting time, $\bar{t}_{s2}$, as a function of dimensionless axial distance, x/D. for various values of initial pressure ratio, p_1/p_o. Diffuser length, L/D= 3. Upstream diaphragm location. Nozzle entrance at 1.81 in.from diaphragm.

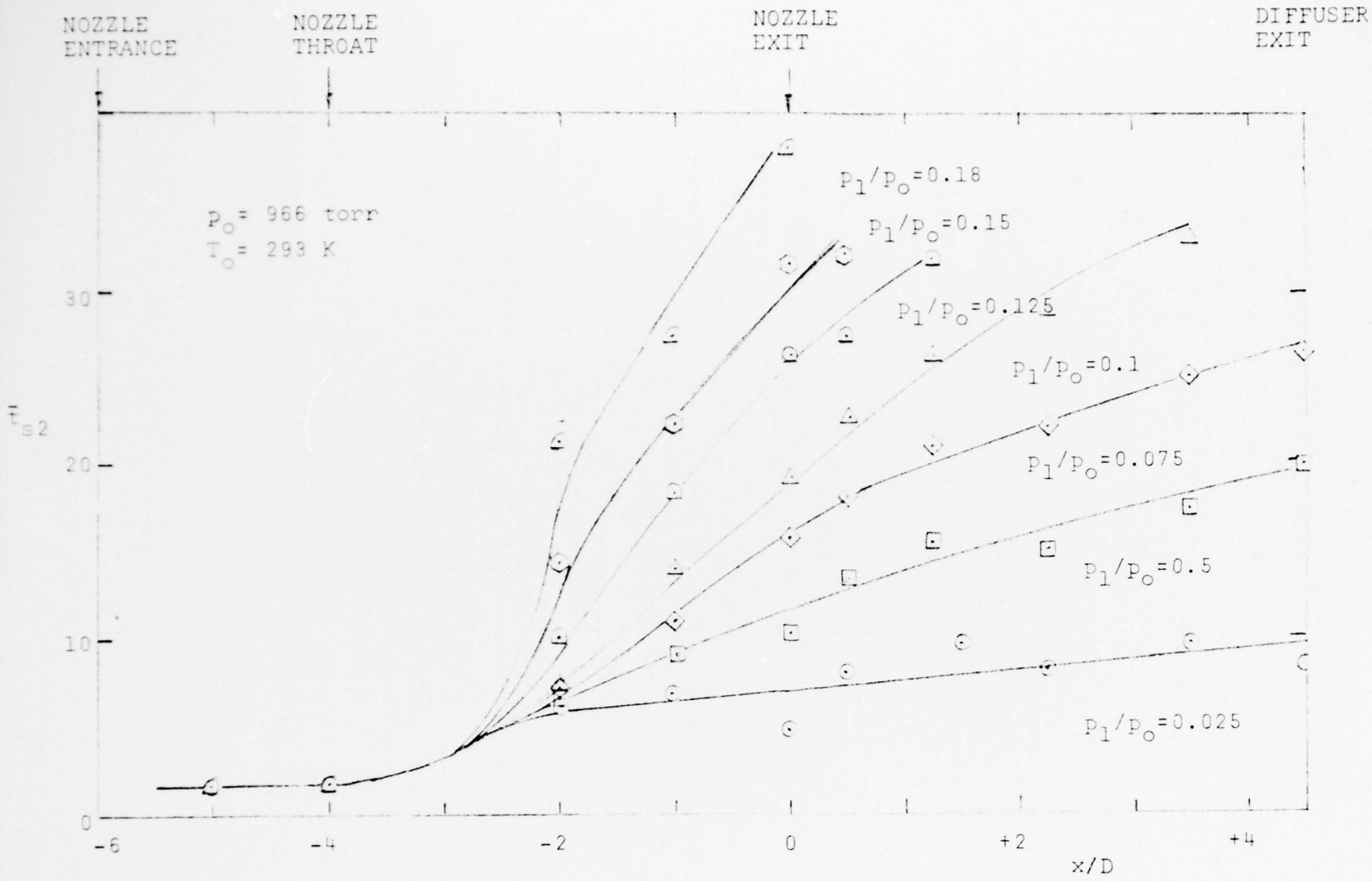

Figure 23. Dimensionless flow starting time, $\bar{t}_{s2}$, as a function of dimensionless axial distance, x/D, for various values if initial pressure ratio, p_1/p_o. Diffuser length, L/D= 4.5. Upstream diaphragm location. Nozzle entrance at 1.81 in. from diaphragm.

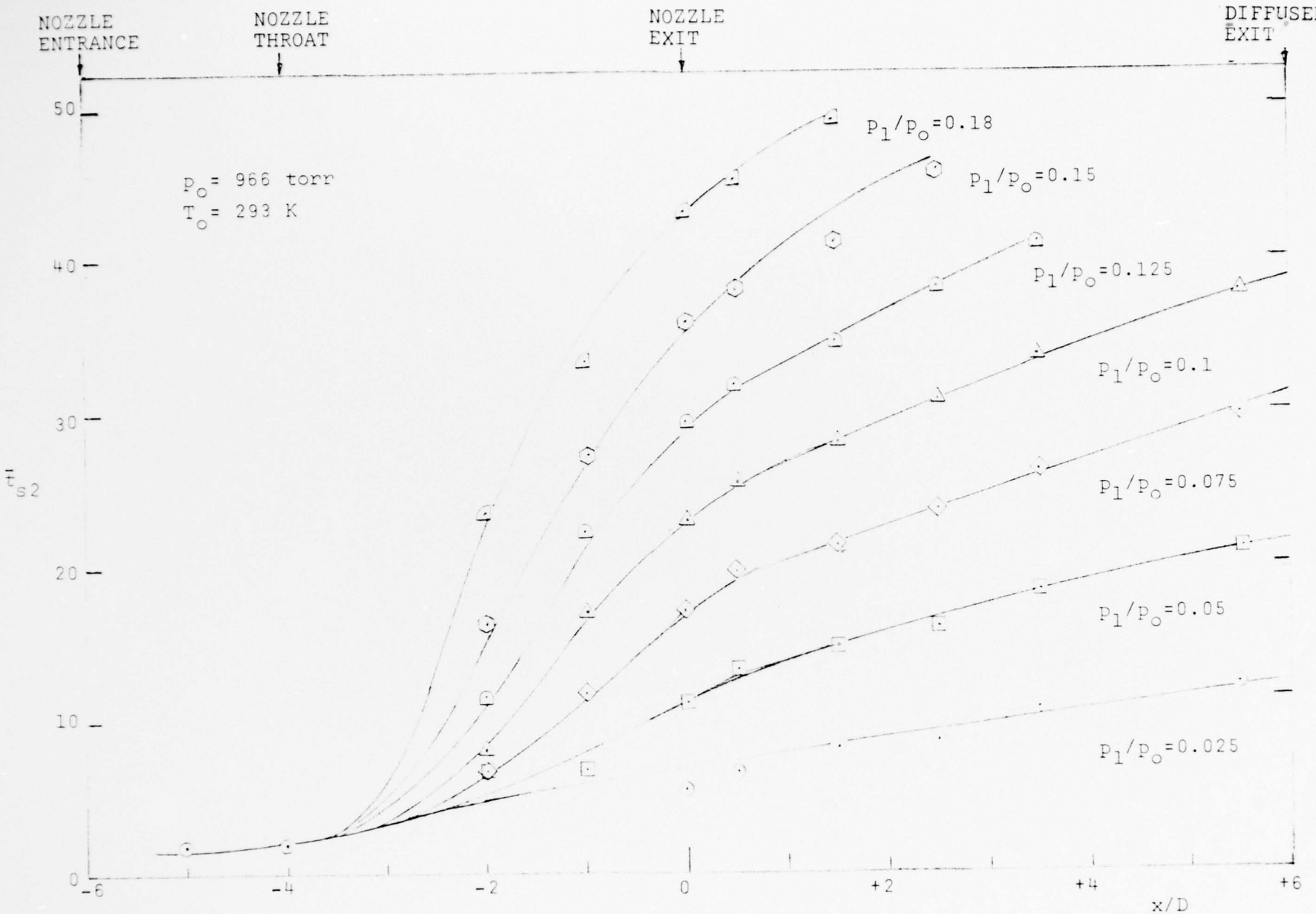

Figure 24. Dimensionless flow starting time, t_{s2}, as a function of dimensionless axial diatance, x/D, for various values of the initial pressure ratio, p_1/p_o. Diffuser length, L/D= 6. Upstream diaphragm location. Nozzle entrance at 1.81 in. from diaphragm.

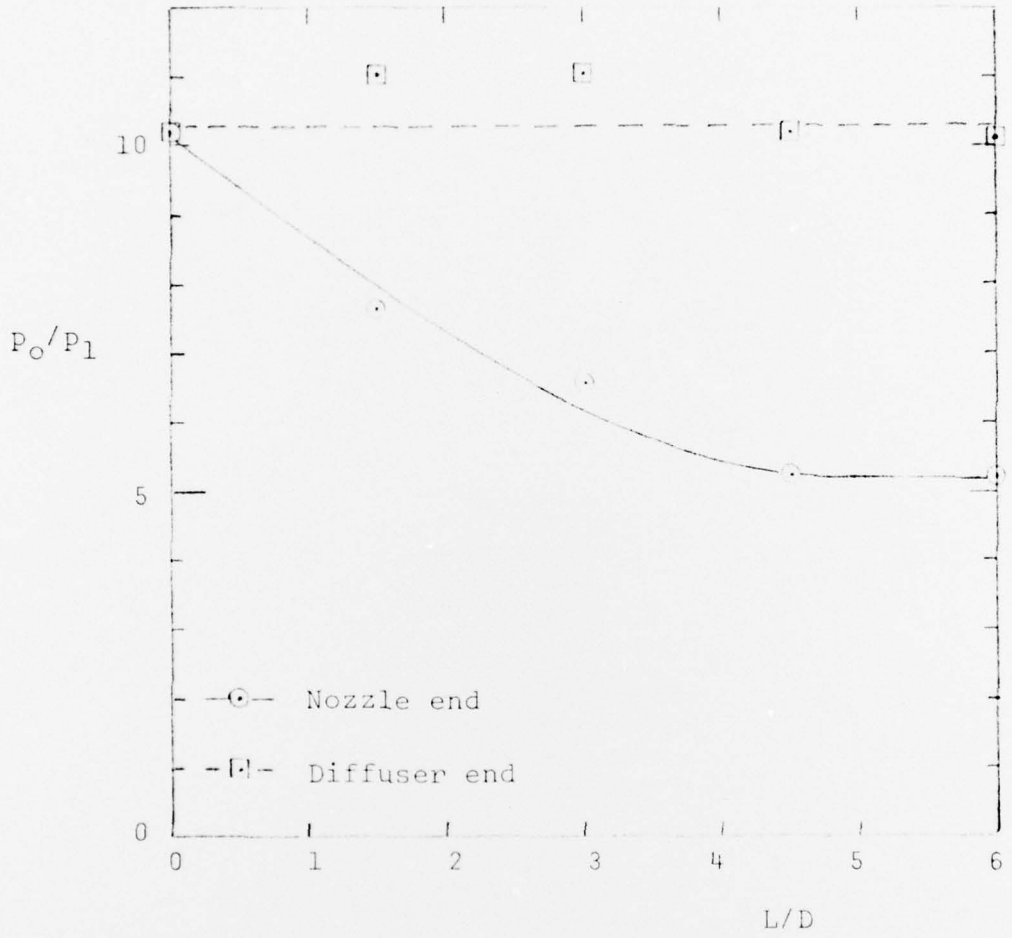

Figure 25. Variation of the initial pressure ratio, p_o/p_1, that permits supersonic flow to start properly in the nozzle and diffuser exits as a function of dimensionless diffuser length, L/D. Upstream diaphragm location. Nozzle entrance at 1.81 in. from diaphragm.

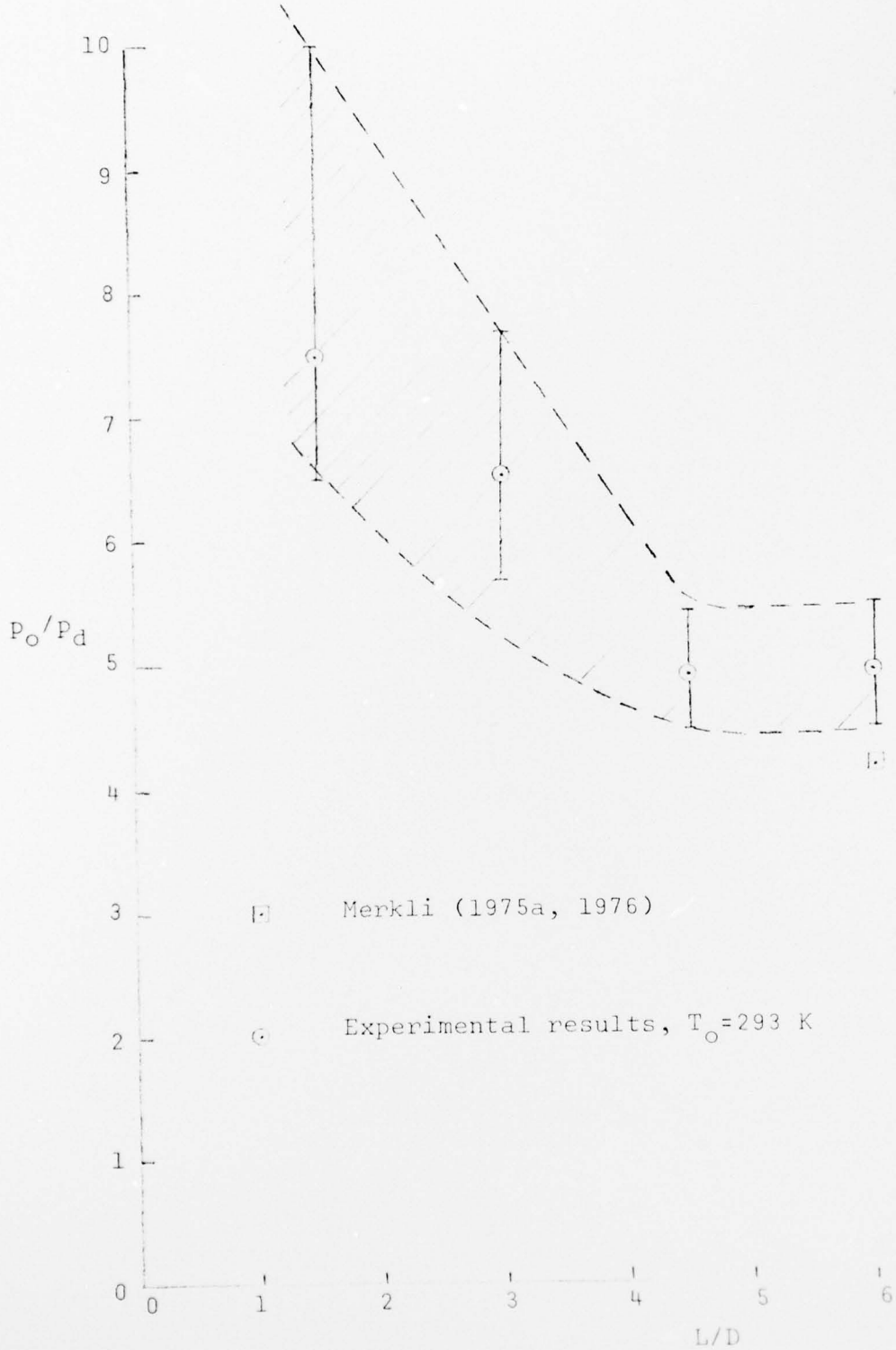

Figure 26. Pressure ratio, p_o/p_d, during the first flow cycle of the Ludwieg tube, as a function of dimensionless diffuser length, L/D. Upstream diaphragm location. Nozzle entrance at 1.81 in. from diaphragm. Comparison between present results and data obtained in a steady continuous tunnel (Merkli, 1975a, 1976).

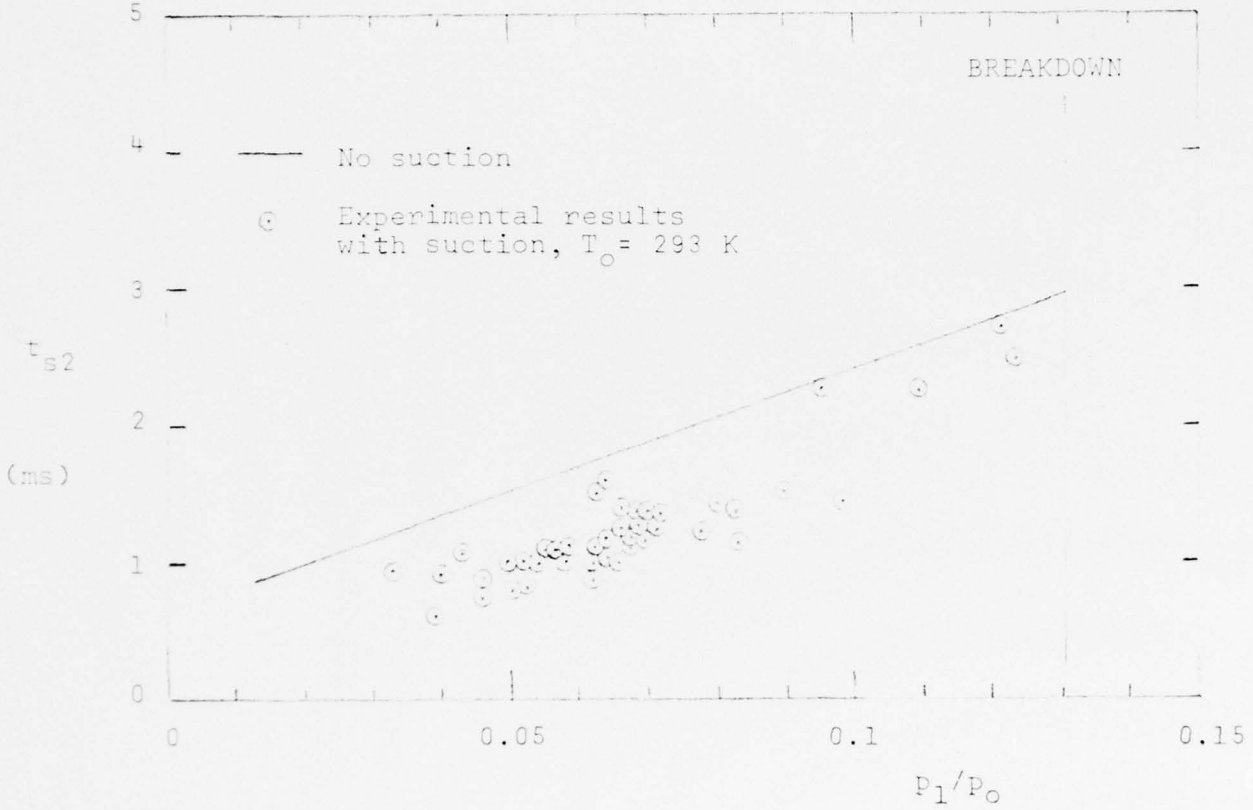

Figure 27. Starting times for the flow at the nozzle exit as a function of initial pressure ratio, p_1/p_o. Diffuser length, L/D = 1.5. Comparison between the results with and without boundary layer suction at nozzle exit. Upstream diaphragm location. Nozzle entrance at 1.81 in. from diaphragm.

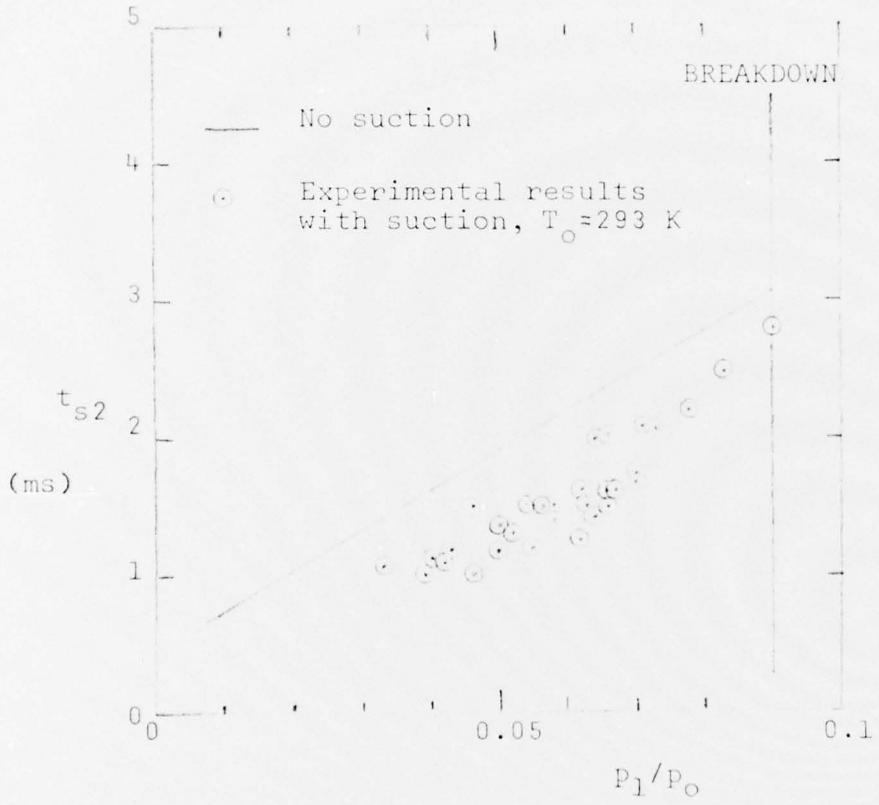

Figure 28. Starting time for the flow at the diffuser exit as a function of initial pressure ratio, p_1/p_o. Diffuser length, L/D= 1.5. Comparison between the results with and without boundary layer suction at nozzle exit. Upstream diaphragm location. Nozzle entrance at 1.81 in. from diaphragm.